

# Expected Bipartite Matching Distance in A $D$ -dimensional $L^p$ Space: Approximate Closed-form Formulas and Applications to Mobility Services

Shiyu Shen<sup>a</sup>, Yuhui Zhai<sup>a</sup>, Yanfeng Ouyang<sup>a</sup>

<sup>a</sup>*Department of Civil and Environmental Engineering, University of Illinois at Urbana-Champaign, Urbana, IL 61801, USA*

---

## Abstract

The bipartite matching problem has been at the core of many theoretical or practical challenges. Although many well-known algorithms can solve each bipartite matching problem instance efficiently, it remains an open question how one could estimate the expected optimal matching distance for arbitrary numbers of randomly distributed vertices in a  $D$ -dimensional  $L^p$  space (referred to as a random bipartite matching problem, or RBMP, in the literature). This paper proposes an analytical model with closed-form formulas (without statistical curve-fitting) that estimate both the probability distribution and expectation of the optimal matching distance of RBMP. Simpler asymptotic approximations of the formulas are also developed for some special cases. A series of Monte-Carlo simulation experiments are conducted to verify the accuracy of the proposed formulas under varying numbers of bipartite vertices, varying number of dimensions, and varying  $L^p$  distance metrics. These proposed distance estimates could be key for strategic performance evaluation and resource planning in a wide variety of application contexts. To illustrate their usefulness, we focus on mobility service systems where matches must be made between customers and service vehicles that are randomly distributed over time and space. We show how the proposed distance formulas provide a theoretical foundation for the empirically assumed Cobb-Douglas matching function for taxi systems, and reveal conditions under which the matching function can be suitable. Our formulas can also be easily incorporated into optimization models to select taxi operation strategies (e.g., whether newly arriving customers shall be instantly matched or pooled into a batch for matching). Agent-based simulations are conducted to verify the predicted performance of the demand pooling strategy for two types of e-hailing taxi systems. The results not only demonstrate the accuracy of the proposed model estimates under various service conditions, but also offer valuable managerial insights for service operators to optimize their strategies.

*Keywords:* Bipartite matching, matching distance, closed-form estimation, random, shared mobility, demand pooling,  $D$ -dimensional space

---

## 1. Introduction

The bipartite matching problem is a fundamental problem in the field of applied mathematics and combinatorial optimization (Asratian et al., 1998). In a bipartite graph, vertices are divided into two distinct subsets, and edges exist only between vertices of different subsets. The objective is to identify an optimal subset of these edges that match the vertices into disjoint pairs (i.e., no two selected edges share a common vertex). The bipartite matching problem has multiple types of variations. The most well-known one might be the maximum/minimum weight bipartite matching

problem, where each edge carries a weight and we seek the matching with the maximum/minimum total weight. If the two subsets of vertices have equal cardinality, we refer to this bipartite graph as balanced. A matching is considered perfect if it covers every vertex; otherwise, if the matching covers only one subset of vertices in an unbalanced bipartite graph, it is said to saturate that particular subset of vertices.

These variations of the bipartite matching problem are very versatile and they have been applied to a variety of theoretical or practical challenges. In the field of physics, the matching solutions can be used to capture important properties of various disordered complex systems, such as identifying the patterns and energy configurations of atomic magnets in spin glass systems (Mézard and Parisi, 1985). In the field of biology, the problem can be used to describe interactions between species in an ecosystem (Simmons et al., 2019), or to analyze pairwise protein-protein interactions (Tanay et al., 2004). In the field of computer science, similar matching problems are formulated for graph-based pattern recognition systems to map the underlying data structures of images/signals to their features/labels (Yu et al., 2020); or for the emerging social media and e-commerce platforms to capture user/information interactions among distinct socioeconomic groups (Zhou et al., 2007; Wu et al., 2022).

In particular, bipartite matching problems are widely applicable to many transportation/mobility systems, where one fundamental challenge is to find matches between travel demand and resource supply over time (e.g., a planning horizon) and space (e.g., a service region). For instance, a bipartite matching problem can be used to address the operations of multiple elevators in a tall building, where customers arrive randomly at different floors and are matched to one of the elevators — All the points of interest would be distributed in a one-dimensional space. In two- or three-dimensional spaces, the problem can be used to describe how surface courier vehicles and idle taxis, or freight drones and passenger aerial vehicles, are matched to their customers in a city. In particular, the latter examples have received a lot of attention, as ride-hailing services for passengers (e.g., as those offered by Transportation Network Companies, TNCs) and freight (e.g., as those offered by courier service companies) are booming all over the world. In their typical operations, customers and vehicles evolve in the system as random points in a service region, and the service platform periodically (e.g., every a few seconds) makes vehicle dispatch and allocation decisions to best serve the customers. In each decision epoch, the system captures a snapshot of its current state to gather information on both idle vehicles (e.g., locations) and new customers (e.g., origin and destination locations, and the elapsed waiting time). Subsequently, a bipartite graph is constructed, where one subset of vertices include all idle vehicles, and the other subset all new customer origins. Weights of the edges could be based on distance (or travel cost, time) and the customers' priority. Matches are then optimized by the platform based on a predefined objective, such as minimizing the total matching distances for pickups (between the vehicles and the customer origins). Any unmatched customers either are assumed lost, or could be retained and moved into the customer pool for the next decision epoch.

This bipartite matching scheme stands out for its ease of computation and implementation. For each decision epoch, the associated problem instance can be solved quickly using linear programming methods or algorithms. For example, many well-known combinatorial optimization algorithms, such as the Hungarian algorithm (Kuhn, 1955), Jonker–Volgenant algorithm (Jonker and Volgenant, 1987), and their variations, can generate near-optimal solutions in polynomial time. Even those more advanced machine-learning based algorithms, as reviewed in (Zhang et al., 2023), can effectively solve these problems within a relatively short time. Hence, for real-time operational

purposes, these state-of-the-art computational techniques are sufficient to be implemented by the operators.

For strategic planning, however, the operators usually need to estimate the service efficiency under a large number of possible realizations of supply and demand scenarios (e.g., different vehicle and customer distributions), rather than finding exact vehicle-customer matches for one particular problem instance. The average matching distance between the vehicles and the customer origins, also commonly referred to as the “deadheading” distance, stands as a key indicator of service efficiency. It indicates the “unproductive” efforts made by both customers (i.e., waiting for pickup) and vehicles (i.e., running empty) within the mobility system. Understanding the relationship between the average matching distance and vehicle/customer distribution can help improve service efficiency in many ways. Operators, for example, often need to set standards for operation, such as determining the time between consecutive decision epochs (i.e., pooling interval). A longer pooling interval may lead to more customers/vehicles appearing in one matching problem instance, potentially reducing the resulting matching distance. However, it also implies that customers need to wait longer to find a match. Finding a balance between these conflicting objectives and identifying the optimal operational standard require knowledge of this quantitative relationship. Moreover, operators often deploy new tactical-level strategies to further enhance their service efficiency. For example, they may swap an already-matched vehicle to a customer with another better candidate vehicle (with a shorter matching distance) whenever feasible (Ouyang and Yang, 2023; Shen and Ouyang, 2023). Analyzing the effectiveness of these strategies (often measured by the reduction in matching distance) under various vehicle/customer distributions also requires such knowledge.

The above needs for strategic planning give rise to a stochastic version of the bipartite matching problem with the following key features: (i) both subsets of vertices are randomly distributed, drawn from some given probability distributions with certain densities, within a given bounded domain of  $D$  spatial dimensions; (ii) the weight on each edge is determined by the distance between the respective vertices according to a specific  $L^p$  metric; (iii) For each realization of random vertices in one problem instance, an optimal matching solution is to be found that primarily minimizes the total weights, and then secondarily, yields the maximum cardinality that saturate the smaller subset of vertices. In this study, we refer to such a problem as the “Random Bipartite Matching Problem (RBMP) in a  $D$ -dimensional  $L^p$  Space.” We are particularly interested in identifying the “average properties” of the optimal matching solution (e.g., to estimate the average “optimal matching distance” per vertex pair).

To the best of our knowledge, estimating the expected “optimal matching distance” for RBMP remains a challenging task. While each random realization of RBMP can be addressed as a deterministic bipartite matching problem, and one could use the state-of-the-art techniques (as those employed by the TNCs) to solve a sufficiently large number of problem instances and produce statistical/simulated results, this process may pose computational challenges and consume considerable time. Moreover, the outcomes may lack the depth of analytical insights. In many cases, analytical models are favored for their efficiency, and they can provide more analytical insights as compared to simulated results, such as those developed in Daganzo et al. (2020) and Ouyang et al. (2021) for estimating several key performance metrics (e.g., the expected vehicle distance traveled) for mobility services given certain operational standards. Moreover, this type of analytical models can be incorporated into the development of more comprehensive optimization/equilibrium models, helping the operators or regulators in optimizing their service offerings to achieve higher service

efficiency or social welfare (Zha et al., 2016; Ouyang et al., 2021; Liu and Ouyang, 2021, 2023). However, as outlined in the literature review, existing analytical models and formulas for estimating matching distances in RBMP have limited applicability to general problem settings. They are applicable only to scenarios such as: (i) the densities of point distributions are (nearly) equal; or (ii) the number of dimensions is limited to only one or two; or (iii) the distance/cost is measured by only Euclidean metric. More importantly, many of these studies primarily focus on identifying asymptotic approximations (or bounds), with proposed formulas still requiring statistical analysis for coefficient fitting. Additionally, they mainly focused on estimating only the expectation of the “optimal matching distance,” lacking specific insights into its distribution.

In response to these challenges, this paper introduces an analytical model with closed-form formulas (without statistical curve-fitting) to estimate both the distribution and expectation of the optimal matching distance for RBMP in a  $D$ -dimensional  $L^p$  Space. Simpler asymptotic approximations of the formula for estimating the expected distance are developed for some special cases. The proposed distance estimates could be key for strategic performance evaluation and resource planning in real-world problems. Particularly in the context of mobility services, the approximated formulas can provide a theoretical explanation regarding the applicability of the empirically assumed Cobb-Douglas meeting function under specific conditions, and provide insights into how some of its parameter values could be set. The formulas can also be integrated into optimization models to determine the best operational strategies (e.g., duration of demand pooling intervals) for e-hailing services across a range of service conditions (e.g., varying demand rates and fleet sizes).

To verify the accuracy of the proposed distance formulas, a set of Monte-Carlo simulations are conducted for a range of most common spatial dimensions and distance metrics for real-world applications (e.g., on-demand mobility problems). The results indicate that our general model can provide accurate RBMP distance estimations with any numbers of bipartite vertices in the metric spaces. In addition, a series of agent-based simulations are conducted to validate the optimal demand pooling strategy for two settings of e-hailing taxi systems. The results indicate that the model estimates match quite well with the simulation measurements under all considered settings. The findings also provide managerial insights on the suitability of instant customer matching, especially in a taxi system with a sufficiently large fleet; demand pooling can be beneficial under certain conditions, especially when the system with a small fleet has been in the middle of an inefficient equilibrium.

The remainder of this paper is organized as follows. Section 2 provides a review of the related literature. Section 3 presents the general model of RBMP and our general formula for the expected matching distance. Section 4 derives a set of approximations of the general formula, as well as the conditions under which they are suitable. Section 5 shows how the proposed formulas can be applied, as an example, to improve on-demand mobility systems. Section 6 presents numerical experiments. Finally, Section 7 offers concluding remarks and suggestions for future research.

## 2. Literature Review

Statistical physicists and mathematicians seem to be among the first to explore a common problem of interest — identifying the “average optimal cost” of stochastic bipartite matching problems. Mézard and Parisi (1985) explored the use of the “replica method” from the mean field theory to derive analytical formulas for the expected optimal cost in a balanced bipartite matching problem, where the weights on the graph edges are i.i.d. from a uniform distribution. The accuracy of their proposed formula was verified in Brunetti et al. (1991) by extensive numerical

experiments, with errors shown to be less than 1% from simulation results for problems of various sizes. Building upon these results, a number of conjectures for other problem variations were proposed. For instance, Parisi (1998) proposed analytical formulas (as conjectures) for balanced matching problems where the edge weights follow an exponential distribution. Then, Coppersmith and Sorkin (1998) and Alm and Sorkin (2002), while still assuming exponentially distributed edge weights, proposed more general conjectures for partial matching in unbalanced bipartite graphs. These conjectures were later proven to be correct by Linusson and Wästlund (2004) and Nair et al. (2005).

These earlier studies paved the way for finding the average optimal cost for a balanced bipartite graph in a bounded Euclidean space, known as the “Random Euclidean Bipartite Matching Problem” (REBMP). When edge weights are drawn as the Euclidean distance between the corresponding random vertices, two notable distinctions stand out: (i) these edge weights follow a triangular distribution, which is much more difficult to analyze than simple uniform or exponential distributions, and (ii) correlations exist among these weights due to the presence of spatial boundaries. Mézard and Parisi (1988) were the first to formally define the Euclidean matching problems and proposed asymptotic approximations to estimate the average optimal costs. Subsequent works (Boniolo et al., 2014; Caracciolo and Sicuro, 2014, 2015) extended these asymptotic analyses and proposed additional approximation formulas (either proven or conjectured) for REBMP with different dimensions or cost metrics. However, these asymptotic approximations were derived under the strong assumption that the number of bipartite vertices approaches infinity, and hence they could only serve as bounds rather than exact estimations when the number of bipartite vertices is small. Caracciolo et al. (2014) formulated several simple parametric models for exact cost estimations under different combinations of spatial dimension and cost metrics, and the key assumption (based on Ajtai et al. (1984); Talagrand (1992)) is that the “leading terms” of the exact optimal cost could be approximated by the product of the asymptotic estimate and a scaling factor. The scaling factor must be estimated from statistical regression or curve fitting on simulated data, except for a few very special settings (e.g., when the edge cost is measured as the square of the Euclidean distance, also known as the “quadratic” cost). Subsequent studies in this field, such as Caracciolo and Sicuro (2015); Ambrosio et al. (2021), also predominantly focused on problems with quadratic costs. When the cost is measured directly by the Euclidean distance, the only relevant results seem to be those presented in Caracciolo et al. (2014), which conjectured that the same scaling-factor-based formula structure holds for balanced problems when the spatial dimension is higher than or equal to three. More recently, Kanoria (2022) showed that such “scaling structure” observed in these static problems can be leveraged, via a hierarchical greedy algorithm, to estimate the bounds of minimum achievable expected cost in imbalanced and dynamic problems. In such dynamic problems, the arrivals/departures of bipartite vertices from one or both subsets follow a stochastic process, and the matches must be made myopically without full information about future arrivals. The bounds were found under special conditions such as when the number of vertices in one subset is fixed. However, they did not provide any formulas for directly estimating the expected matching distance in any case.

In the field of transportation science, a school of literature has independently investigated some similar variants of the RBMP for logistics applications. For instance, Daganzo and Smilowitz (2004) explored a problem known as the Transportation Linear Programming (TLP) problem. They introduced approximate formulas through probabilistic and dimensional analysis, and estimated bounds to the average optimal cost. An exact formula is proposed for balanced 1-dimensional

cases, but for higher-dimensional cases, the formula involves parameters that need to be estimated through statistical regression (i.e., similar to those found in the field of statistical physics). In addition, the formulas are only applicable when the bipartite graph is nearly balanced.

Most of the other studies in this field specifically explored RBMP in a 2-dimensional space. The most fundamental model introduced in Daganzo (1978) estimates the probability distribution and expectation of the minimum matching distance from one random point to a set of random points—a special case of RBMP where the number of vertices in one subset is simply one. For more general matching problems with arbitrary numbers of vertices in the subsets, a widely used model in this field is an assumed Cobb-Douglas formula – called the “matching function” — proposed by Yang et al. (2010). It has been used extensively to estimate the matching rate/distance between customers and vehicles (as two subsets of points) in mobility services (Yang and Yang, 2011; Zha et al., 2016; Zhang et al., 2019). This model is established based on a hypothetical conjecture that vehicle-customer matching rate can be interpreted as the “productivity” of a mobility market, and the parameters in the Cobb-Douglas formula are typically assumed or estimated via statistical regression from simulated or real-world data. Section 5.1 will provide more detailed discussions on this model.

More recently, Lei and Ouyang (2024) developed an analytical model to estimate the expected tour length for visiting a random subset of points within a compact region. Although this study did not specifically address RBMP, it offered insights into ways to identify the expected distance from one random subset of points to another.

In summary, to the best of our knowledge, none of the existing studies have succeeded in deriving exact formulas that can estimate the expected optimal cost to RBMP under general problem settings. Many existing formulas are restricted to special problem settings, such as those related to certain numbers of bipartite vertices (e.g., balanced), limited dimensions (e.g., greater than three), or specific cost metrics (e.g., Euclidean). Most results also require parameter estimation from statistical curve fitting to simulated or real-world data. This paper aims to develop a general model to accommodate problems with arbitrary numbers of bipartite vertices, any number of dimensions, and any  $L^p$  distance metrics. Furthermore, our goal is to derive a closed-form formula supported by sufficient theoretical explanations; i.e., no curve fitting would be needed.

### 3. General Model

#### 3.1. Problem Definition

We begin by formally defining the RBMP in a “unit volume” hyper-ball  $\Omega$  within a  $D$ -dimensional  $L^p$  (Lebesgue) space (i.e.,  $\Omega \subseteq \mathbb{R}^D$ ), where  $D \in \mathbb{Z}^+$  and  $p \in \mathbb{Z}^+$ . The radius of  $\Omega$ , denoted as  $R$ , can be expressed as a function of  $D$  and  $p$  as follows (Olver, 2010):

$$R(D, p) = \frac{\Gamma\left(\frac{D}{p} + 1\right)^{\frac{1}{D}}}{2\Gamma\left(\frac{1}{p} + 1\right)}, \quad (1)$$

where  $\Gamma(z) = \int_0^\infty t^{z-1} e^{-t} dt$  is the gamma function. Two subsets of points, with given cardinalities  $n \in \mathbb{Z}^+$  and  $m \in \mathbb{Z}^+$ , respectively, are independently and uniformly generated within  $\Omega$ . Without loss of generality, we assume  $n \geq m$ . The distance between any two points with coordinates  $(x_1, \dots, x_D)$  and  $(y_1, \dots, y_D)$  is measured by the given  $L^p$  metric as  $\left(\sum_{i=1}^D |x_i - y_i|^p\right)^{\frac{1}{p}}$ .

For each realization of RBMP's point locations (which we call an RBMP- $(D, p, n, m)$  instance), a bipartite graph  $G = (U \cup V; E)$  can be constructed, where  $V$  and  $U$  represent the two subsets of points, where  $|V| = n$  and  $|U| = m$ , and  $E$  represents the set of edges connecting every pair of points  $u \in U$  and  $v \in V$ . The weight on edge  $(u, v) \in E$  is the corresponding  $L^p$  distance, denoted  $\|u, v\|$ . Since we have assumed that  $m \leq n$ , each point  $u \in U$  will find exactly one match  $v(u) \in V$ . The objective is to identify  $\{v(u), \forall u \in U\}$  that minimizes the total distances between the matched points:

$$\min_{\{v(u), \forall u \in U\}} \sum_{u \in U} \|u, v(u)\|, \text{ s.t. } v(u) \neq \emptyset, \forall u \in U \text{ and } v(u_1) \neq v(u_2), \forall u_1 \neq u_2 \in U.$$

Let the optimal match and the corresponding distance for  $u \in U$  be denoted as  $v^*(u)$  and  $\|u, v^*(u)\|$  respectively.

Now we randomly select one point  $\bar{u} \in U$ , and record its optimal matching distance  $\|\bar{u}, v^*(\bar{u})\|$ . This distance is a random variable that depends on the random realization of  $U, V$  and the random selection of  $\bar{u}$ , both of which are governed by parameters  $D, p, n, m$ . We hence denote it  $X_{D,p,n,m}$ . The primary objective of this section is to derive approximate closed-form formulas for the probability distribution and expectation of  $X_{D,p,n,m}$ . For simplicity, we will drop the subscripts and use the notation  $X$  from now on.

It is important to note that, correlation exists (i) among the distribution of distances between points within the underlying metric space, particularly as  $\Omega$  is bounded; (ii) among the matching between two subsets of points, especially when  $m \rightarrow n$ . Obviously, it is non-trivial to address the impacts of such correlation comprehensively. Yet, Mézard and Parisi (1988) has shown that such impacts for  $m = n$  diminish as  $D \rightarrow \infty$  and remain relatively small even for finite  $D$ . As such, for modeling simplicity, we make the assumption, in our general analysis, that all the points within each subset (i.e.,  $U$  or  $V$ ) are, respectively, probabilistically identically and independently distributed (i.i.d.) within  $\Omega$ , and identically and independently matched with the points in the other subset.

### 3.2. General Results

Notably, from the perspective of a randomly sampled point  $\bar{u} \in U$  in one problem instance, its optimal match  $v^*(\bar{u})$  may be its  $k_{\text{th}}$  nearest neighbor among those in set  $V$ , where  $k \geq 1$ . Estimating the distribution and expectation of  $X$  involves two main steps: (i) deriving the probability of  $\bar{u}$  to be matched with its  $k_{\text{th}}$  nearest neighbor, denoted as  $P(k)$ , and (ii) estimating the probability distribution and expectation of the corresponding distance from  $\bar{u}$  to that  $k_{\text{th}}$  nearest neighbor, denoted as  $Y_k$ . They will be discussed next.

#### 3.2.1. Probability of being matched to one's $k_{\text{th}}$ nearest neighbour

In this subsection, we derive an approximated formula for  $P(k)$ . For any given problem instance, imagine that we perform a sorting process to the optimal matching  $\{v^*(u), \forall u \in U\}$ , as outlined below: (i) for each point  $u \in U$ , sort all the points in  $V$  into a sequence based on their distance to  $u$  in an ascending order,  $K_u[v] : V \rightarrow \{1, \dots, n\}$ , and find the position of  $v^*(u)$  in this sequence, denoted  $K_u^*$ ; (ii) sort the points in  $U$  based on the value of  $K_u^*$  in an ascending order,  $I[u] : U \rightarrow \{1, \dots, m\}$ , and break ties arbitrarily. A matrix of size  $m \times n$  can be constructed by sequentially filling each row with the corresponding sorted points in  $V$ . Every  $v$  appears exactly once in each row, with row and column indices  $I[u]$  and  $K_u[v]$  respectively. Since the sorting process is applied

to an optimal matching solution, two facts must hold: (i) the column index of  $v^*(u)$  must be smaller or equal to  $u$ 's row index (i.e.,  $K_u^* \leq I[u]$ ), and (ii) every  $v$  in that row that satisfies  $K_u[v] < K_u^*$  must be matched to another point in  $U$ . If either fact is violated, the matching solution can be improved by simple point swaps — and hence could not have been optimal.

Despite the sorting process for the points in  $U$ , from the perspective of those in  $V$ , under the i.i.d. assumption, for each row, each  $v$  has an equal probability of being located in any one of the  $n$  columns. Now let's consider the case  $I[\bar{u}] = m$ ; i.e.,  $\bar{u}$  corresponds to the last row of this  $m \times n$  matrix. The value of  $K_{\bar{u}}^*$  equals  $k \in \{1, \dots, m-1\}$  when (a) all those in row  $m$ 's first  $k-1$  columns are among the  $m-1$  points in  $V$  that are matched with the  $m-1$  other points in  $U$ , which occurs with a probability of  $\left(\frac{m-1}{n}\right)^{k-1}$ ; and (b) the  $k$ -th column is not, which occurs with a probability of  $\left(1 - \frac{m-1}{n}\right)$ . The special case  $K_{\bar{u}}^* = m$  occurs as long as condition (a) is satisfied, with a probability of  $\left(\frac{m-1}{n}\right)^{m-1}$ , since condition (b) is automatically satisfied when (a) holds. These results are summarized as follows:

$$\Pr\{K_{\bar{u}}^* = k \mid I[\bar{u}] = m\} \approx \begin{cases} \left(\frac{m-1}{n}\right)^{k-1} \left(1 - \frac{m-1}{n}\right), & \forall k \in \{1, \dots, m-1\}, \\ \left(\frac{m-1}{n}\right)^{m-1}, & k = m. \end{cases} \quad (2)$$

Then, let's consider the other rows, e.g., any  $i \in \{1, \dots, m-1\}$ . Instead of directly analyzing it, we focus on a “truncated” bipartite matching problem with the original  $V$  but a subset of  $i$  points in  $U$  that correspond to the first  $i$  rows in the original  $m \times n$  matrix. If we solve this truncated problem instance and do the same sorting process to its optimal matching, Equation (2) still holds for its last row  $i$  (the probability of  $K_{\bar{u}}^{**} = k$  given  $I[\bar{u}] = i$ ), as long as  $m$  is replaced by  $i$  everywhere. As such, for all  $i \in \{1, \dots, m\}$ , we have:

$$\Pr\{K_{\bar{u}}^{**} = k \mid I[\bar{u}] = i\} \approx \begin{cases} \left(\frac{i-1}{n}\right)^{k-1} \left(1 - \frac{i-1}{n}\right), & k \in \{1, \dots, i-1\}, \\ \left(\frac{i-1}{n}\right)^{i-1}, & k = i. \end{cases} \quad (3)$$

Note here the expected value of  $K_{\bar{u}}^{**}$  given  $I[\bar{u}] = i$  in the truncated problem shall be no larger than the expected value of  $K_{\bar{u}}^*$  given  $I[\bar{u}] = i$  of the original problem (because there is less competition from other points in  $U$ ). In addition, every point in  $U$  has the same probability  $\frac{1}{m}$  to be in the  $i$ <sub>th</sub> position in the sorted optimal solution matrix; i.e.,  $\Pr\{I[\bar{u}] = i\} = \frac{1}{m}$ . As such, we have  $\mathbb{E}[K_{\bar{u}}^* \mid I[\bar{u}] = i] \geq \mathbb{E}[K_{\bar{u}}^{**} \mid I[\bar{u}] = i] = \sum_{k=1}^i k \cdot \Pr\{K_{\bar{u}}^{**} = k \mid I[\bar{u}] = i\}$ , and hence:

$$\frac{1}{m} \sum_{i=1}^m \sum_{k=1}^i k \cdot \Pr\{K_{\bar{u}}^* = k \mid I[\bar{u}] = i\} = \mathbb{E}[K_{\bar{u}}^*] \geq \mathbb{E}[K_{\bar{u}}^{**}] = \frac{1}{m} \sum_{i=1}^m \sum_{k=1}^i k \cdot \Pr\{K_{\bar{u}}^{**} = k \mid I[\bar{u}] = i\}. \quad (4)$$

The probability estimates in Equation (3) is only approximate because it builds upon the i.i.d. assumption. We next show that under the same i.i.d. assumption, these estimates can be achieved through the following greedy matching process. Randomly check a point  $u \in U$ , sort the points in  $V$  based on descending proximity and match  $u$  with its nearest neighbor that has not been matched previously checked points in  $U$ . The process ends when all points in  $U$  have found their matches. This results in a new matrix of size  $m \times n$ , whose  $i$ <sub>th</sub> row corresponds to the  $i$ <sub>th</sub> checked point. Let  $K_{\bar{u}}^o$  denote the column index of the match  $v(\bar{u})$  found for a random point  $\bar{u}$ . Under the i.i.d. assumption, each nearby point  $v$  of  $\bar{u}$  has an equal probability of  $\frac{i-1}{n}$  to have been matched to one



of the preceding  $i - 1$  points in  $U$ . The conditional probability for  $\Pr\{K_{\bar{u}}^o = k \mid I[\bar{u}] = i\}$  shall be the same as the right hand side of Equation (3); i.e.,

$$\Pr\{K_{\bar{u}}^o = k \mid I[\bar{u}] = i\} = \Pr\{K_{\bar{u}}^{**} = k \mid I[\bar{u}] = i\}. \quad (5)$$

Note here the expected value of  $K_{\bar{u}}^o$  in this new matrix shall be no smaller than the expected value of  $K_{\bar{u}}^*$  in the optimal solution matrix (because the above greedy matching process would generate a “feasible” solution). As such, we have:

$$\mathbb{E}[K_{\bar{u}}^*] \leq \mathbb{E}[K_{\bar{u}}^o] = \frac{1}{m} \sum_{i=1}^m \sum_{k=1}^i k \cdot \Pr\{K_{\bar{u}}^o = k \mid I[\bar{u}] = i\}. \quad (6)$$

Equations (4)-(6) jointly indicate that the inequalities in Equation (4) could be rewritten as (approximate) equations when  $\Pr\{K_{\bar{u}}^* = k \mid I[\bar{u}] = i\}$  is given by the right hand side of Equation (3). This probability formula yields an unbiased estimate of  $\mathbb{E}[K_{\bar{u}}^*]$ . As such, we propose to compute  $P(k)$  for all  $k \in \{1, \dots, m\}$  based on Equation (3), as follows:

$$\begin{aligned} P(k) &= \sum_{i=1}^m \Pr\{K_{\bar{u}}^* = k \mid I[\bar{u}] = i\} \Pr\{I[\bar{u}] = i\} \\ &\approx \frac{1}{m} \left(\frac{k-1}{n}\right)^{k-1} + \frac{1}{m} \sum_{i=k+1}^m \left(\frac{i-1}{n}\right)^{k-1} \left(1 - \frac{i-1}{n}\right). \end{aligned} \quad (7)$$

### 3.2.2. Distance to one's $k_{th}$ nearest neighbour

Bhattacharyya and Chakrabarti (2008) came up with an estimate for the expected value of  $Y_k$  in a  $D$ -dimensional Euclidean space. Here, we generalize the result to  $L^p$  space with a simpler new proof, which also yields its cumulative distribution function (CDF).

**Lemma 1.** *The CDF of  $Y_k$ , denoted as  $F_{Y_k}(x)$  for  $k \in \{1, \dots, n\}, x \in [0, R(D, p)]$ , can be expressed as:*

$$F_{Y_k}(x) = \frac{\Gamma(n+1)}{\Gamma(k)\Gamma(n-k+1)} \int_0^{\left[\frac{x}{R(D,p)}\right]^D} t^{k-1}(1-t)^{n-k} dt, \quad (8)$$

where  $R(D, p)$  is given by Equation (1).

*Proof.* By definition of CDF,  $F_{Y_k}(x) = 1 - \Pr\{Y_k \geq x\}, \forall x \in [0, R(D, p)]$ . Since the  $n$  points in  $V$  are uniformly and independently distributed, if again we ignore the boundary and assume that the “generic” reference point is at the center of the given hyper-ball, the probability that any single point is inside an interior hyper-ball of radius  $x$  is given by its volume  $\left[\frac{x}{R(D,p)}\right]^D$ . The probability for exactly  $q \in \{0, \dots, k-1\}$  of these  $n$  points to be inside this interior hyper-ball is given by a binomial distribution. Hence, we have

$$\Pr\{Y_k \geq x\} = \sum_{q=0}^{k-1} \binom{n}{q} \left\{ \left[\frac{x}{R(D,p)}\right]^D \right\}^q \left\{ 1 - \left[\frac{x}{R(D,p)}\right]^D \right\}^{n-q}.$$

The above partial sum of binomial probabilities is well known to be equivalent to an incomplete beta integral, or the CDF of a  $F$ -distribution (Jowett, 1963):  $F(k-1; n, \left[\frac{x}{R(D,p)}\right]^D) =$

$1 - I_{\left\{\left[\frac{x}{R(D,p)}\right]^D\right\}}(n - k + 1, k)$ . Here  $I_z(a, b) = \frac{B(z; a, b)}{B(a, b)}$  is the regularized beta function, in which  $B(a, b) = \int_0^1 t^{a-1}(1-t)^{b-1} dt = \frac{\Gamma(a)\Gamma(b)}{\Gamma(a+b)}$  is the beta function, and  $B(z; a, b) = \int_0^z t^{a-1}(1-t)^{b-1} dt$  is the incomplete beta function. As such,

$$\Pr\{Y_k \geq x\} = 1 - \frac{\Gamma(n+1)}{\Gamma(k)\Gamma(n-k+1)} \int_0^{\left[\frac{x}{R(D,p)}\right]^D} t^{k-1}(1-t)^{n-k} dt.$$

This yields Equation (8).  $\square$

**Lemma 2.** *The expectation of  $Y_k$ , for  $k \in \{1, 2, \dots, n\}$ , can be expressed as:*

$$E[Y_k] = \frac{\Gamma(k + \frac{1}{D})\Gamma(n+1)}{\Gamma(k)\Gamma(n + \frac{1}{D} + 1)} R(D, p), \quad (9)$$

where  $R(D, p)$  is given by Equation (1).

*Proof.* Given  $F_{Y_k}(x)$  from Equation (8),  $E[Y_k]$  the integral of  $x \cdot dF_{Y_k}(x)$  over all values of  $x \in [0, R(D, p)]$ , as follows:

$$E[Y_k] = \frac{\Gamma(n+1)}{\Gamma(k)\Gamma(n-k+1)} \int_0^{R(D,p)} x \cdot d \left( \int_0^{\left[\frac{x}{R(D,p)}\right]^D} t^{k-1}(1-t)^{n-k} dt \right).$$

We substitute  $w = \left[\frac{x}{R(D,p)}\right]^D$ , such that  $x = R(D, p)w^{\frac{1}{D}}$ , and apply the Leibniz integral rule:

$$d \left( \int_0^w t^{k-1}(1-t)^{n-k} dt \right) = w^{k-1} (1-w)^{n-k} dw.$$

Then,

$$\begin{aligned} E[Y_k] &= \frac{\Gamma(n+1)}{\Gamma(k)\Gamma(n-k+1)} \int_0^1 R(D, p)w^{\frac{1}{D}} \cdot w^{k-1}(1-w)^{n-k} dw \\ &= \frac{\Gamma(n+1)}{\Gamma(k)\Gamma(n-k+1)} R(D, p) B \left( k + \frac{1}{D}, n - k + 1 \right) = \frac{\Gamma(k + \frac{1}{D})\Gamma(n+1)}{\Gamma(k)\Gamma(n + \frac{1}{D} + 1)} R(D, p). \end{aligned}$$

This completes the proof.  $\square$

### 3.2.3. The general formula

Now we are ready to present our general formulas. For a randomly sampled  $\bar{u}$  in a randomly sampled RBMP- $(D, p, n, m)$ , it has probability  $P(k)$  to be matched to its  $k_{\text{th}}$  nearest neighbor, and the corresponding matching distance is  $Y_k$ . Considering all possible  $k \in \{1, \dots, m\}$ ,  $\Pr\{X = x\} = \sum_{k=1}^m \Pr\{Y_k = x\}P(k)$ . The results are summarized in the following proposition.

**Proposition 1.** *The CDF and expectation of  $X$ , denoted as  $F_X(x)$  and  $E[X]$ , respectively, can be*

expressed as follows:

$$F_X(x) = \sum_{k=1}^m P(k) F_{Y_k}(x) \approx \frac{1}{m} \sum_{i=1}^m \left[ \sum_{k=1}^i \left( \frac{i-1}{n} \right)^{k-1} \left( 1 - \frac{i-1}{n} \right) F_{Y_k}(x) + \left( \frac{i-1}{n} \right)^i F_{Y_i}(x) \right], \quad (10)$$

where  $F_{Y_k}(x)$  is given by Equation (8), and

$$E[X] = \sum_{k=1}^m P(k) E[Y_k] \approx \frac{R(D, p) \Gamma(n+1)}{m \Gamma(n + \frac{1}{D} + 1)} \sum_{i=1}^m \left[ \sum_{k=1}^i \left( \frac{i-1}{n} \right)^{k-1} \left( 1 - \frac{i-1}{n} \right) \frac{\Gamma(k + \frac{1}{D})}{\Gamma(k)} + \left( \frac{i-1}{n} \right)^i \frac{\Gamma(i + \frac{1}{D})}{\Gamma(i)} \right]. \quad (11)$$

The expected matching distance  $E[X]$ , as presented in closed-form in Equation (11), is referred to as our “general formula” and is applicable for all  $D \in \mathbb{Z}^+$ ,  $p \in \mathbb{Z}^+$ ,  $n \in \mathbb{Z}^+$ ,  $m \in \mathbb{Z}^+$ ,  $n \geq m$ . Note here  $p$  only appears in  $R(D, p)$  outside of the double summations, which decrease monotonically with  $p$ . This indicates that, for different  $p$ , the value of  $E[X]$  varies only by a constant multiplicative factor, and should decrease monotonically with  $p$ . This sheds insights on a simple relationship between the distance metric and the expected matching distance. Additionally, we observe that all terms associated with  $D$ , i.e.,  $R(D, p)$ ,  $\frac{\Gamma(k + \frac{1}{D})}{\Gamma(k + \frac{1}{D} + 1)}$ ,  $\frac{\Gamma(i + \frac{1}{D})}{\Gamma(i + \frac{1}{D} + 1)}$  all increase with  $D$ , and hence  $E[X]$  should increase monotonically with  $D$  as well.

While the impacts of  $m$  and  $n$  cannot be easily seen from Equation (11), it shall be inferred that  $E[X]$  decreases monotonically with  $n$  and increases monotonically with  $m$ , because the vertices in the smaller subset are “competitors” while those in the larger subset are their “targeted resources.” For the special case where  $m = 1$ , note  $0^0 = 1$  and hence Equation (11) reduces to

$$E[X] = \frac{R(D, p) \Gamma(n+1) \Gamma(1 + \frac{1}{D})}{\Gamma(n + \frac{1}{D} + 1)}. \quad (12)$$

More generally, Equation (11) involves double summations and gamma functions that may impose computational challenges, particularly for large values of  $n$  and  $m$ . In the next section, we develop much simpler closed-form asymptotic approximations which not only reveal managerial insights but also can be more suitable for practical use.

#### 4. Asymptotic Approximations of $E[X]$ when $n \gg 1$

In this section, we present a series of approximations for  $E[X]$  and estimate their corresponding error bounds. First, we recall from the well-known Stirling’s approximation that when  $z \gg 1$ , the gamma function satisfies

$$\frac{\Gamma(z + \frac{1}{D})}{\Gamma(z)} \approx z^{\frac{1}{D}}. \quad (13)$$

The following lemma presents error bounds of this approximation:

**Lemma 3.** For  $z \in \mathbb{Z}^+$ ,  $D \in \mathbb{Z}^+$ ,

$$0 \leq z^{\frac{1}{D}} - \frac{\Gamma(z + \frac{1}{D})}{\Gamma(z)} < 1 - \frac{\sqrt{3}}{2}. \quad (14)$$

*Proof.* See Appendix A. □

Then, in Equation (11),  $\frac{\Gamma(n+1)}{\Gamma(n+\frac{1}{D}+1)} \approx (n+1)^{-\frac{1}{D}} \approx n^{-\frac{1}{D}}$  for  $n \gg 1$ , and  $\frac{\Gamma(k+\frac{1}{D})}{\Gamma(k)} \approx k^{-\frac{1}{D}}$  and  $\frac{\Gamma(i+\frac{1}{D})}{\Gamma(i)} \approx i^{-\frac{1}{D}}$  when  $i \geq k \gg 1$ . We introduce a threshold  $\kappa \in \{0, \dots, m\}$  as a user-specified minimal value of  $z$  for the approximation in Equation (13) to be applied. The corresponding approximation, denoted by  $E_\kappa[X]$  becomes the following:

$$E_\kappa[X] = \frac{R(D, p)}{mn^{\frac{1}{D}}} \sum_{i=1}^m \left[ \sum_{k=1}^i \left( \frac{i-1}{n} \right)^{k-1} \left( 1 - \frac{i-1}{n} \right) \left( \mathbf{1}_{k \leq \kappa} \cdot \frac{\Gamma(k+\frac{1}{D})}{\Gamma(k)} + \mathbf{1}_{k > \kappa} \cdot k^{\frac{1}{D}} \right) + \left( \frac{i-1}{n} \right)^i \left( \mathbf{1}_{i \leq \kappa} \cdot \frac{\Gamma(i+\frac{1}{D})}{\Gamma(i)} + \mathbf{1}_{i > \kappa} \cdot i^{\frac{1}{D}} \right) \right]. \quad (15)$$

The following proposition gives the error bounds of this approximation.

**Proposition 2.** *When  $n \gg 1$ ,  $\kappa \in \{0, \dots, m\}$ ,*

$$0 \leq E_\kappa[X] - E[X] \leq \left( 1 - \frac{\sqrt{3}}{2} \right) R(D, p) \cdot n^{-\frac{1}{D}},$$

and  $\lim_{n \rightarrow +\infty} (E_\kappa[X] - E[X]) \rightarrow 0$  for  $D < \infty$ .

*Proof.* See Appendix B. □

Proposition 2 implies that  $E_\kappa[X]$  is a good approximation of  $E[X]$  when  $n$  is sufficiently large. The value of  $\kappa$  should be chosen to find a good trade-off between accuracy and computation efficiency. Note here setting  $\kappa = m$  yields the most accurate approximation for the general formula, however requires the most computational effort. To the extreme, we may set  $\kappa = 0$ ; i.e., use Equation (13) to approximate all gamma function ratios. This simplest (and yet least accurate) formula becomes the following:

$$E_0[X] = \frac{R(D, p)}{mn^{\frac{1}{D}}} \sum_{i=1}^m \left[ \sum_{k=1}^i \left( \frac{i-1}{n} \right)^{k-1} \left( 1 - \frac{i-1}{n} \right) k^{\frac{1}{D}} + \left( \frac{i-1}{n} \right)^i i^{\frac{1}{D}} \right]. \quad (16)$$

To further simplify this formula, we can rewrite the first term within the square brackets into the difference between two summations from  $k = 1$  to  $\infty$ , as follows:

$$\sum_{k=1}^i \left( \frac{i-1}{n} \right)^{k-1} \left( 1 - \frac{i-1}{n} \right) k^{\frac{1}{D}} = \left( 1 - \frac{i-1}{n} \right) \left[ \sum_{k=1}^{\infty} \left( \frac{i-1}{n} \right)^{k-1} k^{\frac{1}{D}} - \sum_{k=1}^{\infty} \left( \frac{i-1}{n} \right)^{k-1+i} (k+i)^{\frac{1}{D}} \right].$$

Noting  $(1 - \frac{i-1}{n}) \sum_{k=1}^{\infty} \left( \frac{i-1}{n} \right)^{k-1} = 1$ , the second term within the square brackets can also be written into a summation from  $k = 1$  to  $\infty$ , as follows:

$$\left( \frac{i-1}{n} \right)^i i^{\frac{1}{D}} = \left( 1 - \frac{i-1}{n} \right) \sum_{k=1}^{\infty} \left( \frac{i-1}{n} \right)^{k-1} \left( \frac{i-1}{n} \right)^i i^{\frac{1}{D}}.$$

Equation (16) then becomes:

$$\begin{aligned} E_0[X] = & \frac{R(D,p)}{mn^{\frac{1}{D}}} \sum_{i=1}^m \left[ \left(1 - \frac{i-1}{n}\right) \sum_{k=1}^{\infty} \left(\frac{i-1}{n}\right)^{k-1} k^{\frac{1}{D}} \right. \\ & \left. - \left(1 - \frac{i-1}{n}\right) \left(\frac{i-1}{n}\right)^i \sum_{k=1}^{\infty} \left(\frac{i-1}{n}\right)^{k-1} \left((k+i)^{\frac{1}{D}} - i^{\frac{1}{D}}\right) \right]. \end{aligned} \quad (17)$$

By omitting the second term inside the square brackets in Equation (17), and using the polylogarithm function  $\text{Li}_{-\frac{1}{D}}\left(\frac{i-1}{n}\right) = \sum_{k=1}^{\infty} \left(\frac{i-1}{n}\right)^k k^{\frac{1}{D}}$  to substitute the first term, we obtain the following formulation:

$$\hat{E}_0[X] = \frac{R(D,p)}{mn^{\frac{1}{D}}} \left[ 1 + \sum_{i=2}^m \left(\frac{n}{i-1} - 1\right) \text{Li}_{-\frac{1}{D}}\left(\frac{i-1}{n}\right) \right]. \quad (18)$$

For  $D \in \mathbb{Z}^+$ , and  $u \in (0, 1)$ , it is well-known that  $\frac{u}{(1-u)} = \text{Li}_0(u) \leq \text{Li}_{-\frac{1}{D}}(u) \leq \text{Li}_{-1}(u) = \frac{u}{(1-u)^2}$  (Wood, 1992). Let  $u = \frac{i-1}{n}$ , we can get the first two inequalities below:

$$m \leq 1 + \sum_{i=2}^m \left(\frac{n}{i-1} - 1\right) \text{Li}_{-\frac{1}{D}}\left(\frac{i-1}{n}\right) \leq n \sum_{i=1}^m \frac{1}{n-i+1} \leq n \ln\left(\frac{n}{n-m}\right). \quad (19)$$

The last inequality comes from the fact that  $\frac{1}{n-i+1}$  monotonically increases with  $i$ , and hence  $\sum_{i=1}^m \frac{1}{n-i+1} \leq \int_1^{m+1} \frac{1}{n-i+1} di = \ln\left(\frac{n}{n-m}\right)$ . This directly leads to the following lemma.

**Lemma 4.** *When  $n \gg m \geq 1$ ,*

$$\frac{R(D,p)}{n^{\frac{1}{D}}} \leq \hat{E}_0[X] \leq \frac{R(D,p)}{n^{\frac{1}{D}}} \left(-\frac{n}{m}\right) \ln\left(1 - \frac{m}{n}\right). \quad (20)$$

Lemma 4 further gives us the following proposition.

**Proposition 3.** *When  $n \gg m \geq 1$ ,*

$$0 \leq \frac{\hat{E}_0[X] - E_0[X]}{\hat{E}_0[X]} \leq \max\left\{\left(\frac{m-1}{n}\right)^m, e^{-4}\right\},$$

and  $\lim_{n \rightarrow +\infty} \left(\hat{E}_0[X] - E_0[X]\right) \rightarrow 0$  for  $D < \infty$ .

*Proof.* See Appendix C. □

Proposition 3 suggests that the percentage error between  $\hat{E}_0[X]$  and  $E_0[X]$  must be: (i) strictly less than  $e^{-1}$ , as per Equation (C.3); and (ii) no more than  $e^{-4}$  when  $n \gg m \geq 1$  and  $\lim_{n \rightarrow +\infty} \left(\frac{m-1}{n}\right)^m \rightarrow 0$ . It also implies that  $\hat{E}_0[X]$  can provide a good approximation of  $E_0[X]$  when  $n$  is sufficiently large.

Finally, note that when  $n \gg m \geq 1$ ,  $\ln\left(1 - \frac{m}{n}\right) \approx -\frac{m}{n}$ , and the gap between the two bounds in Equation (20) diminishes. Therefore, we have the following asymptotic approximation.

**Proposition 4.** *When  $n \gg m \geq 1$ ,*

$$\hat{E}_0[X] \approx \frac{R(D, p)}{n^{\frac{1}{D}}}. \quad (21)$$

## 5. Insights and Applications to Mobility Problems

In this section, we apply our proposed formulas to 2-dimensional mobility problems. Using the taxi systems as an example, we first show that our model can be used to provide a theoretical explanation (or justification) on the conditions under which the empirically assumed taxi meeting function in the Cobb-Douglas form (Yang et al., 2010) are suitable, and how some of its parameter values should be set. Then, we demonstrate how our formulas can be integrated into simple optimization models to design the best operational strategies for e-hailing taxi systems.

### 5.1. Cobb-Douglas function as a special case

The meeting function (Yang et al., 2010) is widely applied to the analysis of customer-vehicle matching process in taxi systems. It was originally developed for the street-hailing service, where customers must be picked up by vehicles at predetermined locations, but was later extended to the e-hailing services (Zha et al., 2016). The model says that the steady-state meeting (or “pickup”) rate between  $m$  randomly located waiting customers and  $n$  randomly located idle vehicles, denoted  $M$  [ $\text{tu}^{-1}$ ], is given by the following matching function in the Cobb-Douglas form:

$$M(m, n) = \alpha_0 \cdot m^{\alpha_1} \cdot n^{\alpha_2},$$

where  $\alpha_0$  [ $\text{tu}^{-1}$ ] is a scaling parameter;  $\alpha_1 \in (0, 1]$  and  $\alpha_2 \in (0, 1]$  are unitless elasticities with respect to  $m$  and  $n$ , respectively. From the Little’s formula, one can derive the expected customer waiting time as follows:

$$\frac{m}{M(m, n)} = \alpha_0^{-1} \cdot m^{1-\alpha_1} \cdot n^{-\alpha_2}. \quad (22)$$

Multiplying this waiting time by the vehicle speed gives the expected matching distance  $E[X]$ . If proper units  $\text{du}$  and  $\text{tu}$  are chosen, the value of the area size and vehicle speed of any given service region can both have a value of 1, and hence Equation (22) directly gives the value of  $E[X]$ .

A series of studies have tried to explore the values of parameters  $\alpha_0, \alpha_1, \alpha_2$ , either theoretical or empirical, under different settings. For instance, Yang and Yang (2011) and Zha et al. (2016) argued qualitative that, based on microeconomics theory, the value of  $\alpha_1 + \alpha_2$  should satisfy  $> 1, = 1$  or  $< 1$  based on whether the market exhibits an increasing, constant or decreasing return to scale, while  $\alpha_0$  should depend on the service region’s characteristics (e.g., area size and vehicle speed). In their studies, they simply tested a range of  $\alpha_0$  values, and assumed that  $\alpha_1 = \alpha_2$  (“for symmetry”) with varying values from 0.25 to 0.8. Table 1 gives a summary of their assumed parameter values. These values were chosen purely to demonstrate, in theory, how the market’s economic properties (e.g., service quality and market profitability) could vary under different parameter combinations; no empirical analyses were conducted to validate these choices.

Other studies have tried to calibrate these parameters based on simulated or empirically observed data, normally via linear regression. For example, Yang et al. (2014) was the first to use empirical data, collected from Hong Kong’s street-hailing service statistics in years 1986-2009, to estimate the parameters. Zhang et al. (2019) later used e-hailing service data collected from

Shenzhen in year 2016, and parameter values were estimated with or without the assumption that  $\alpha_1 = \alpha_2$  — Significant differences were found in the estimated parameter values (as shown in Table 1), but this “symmetry” assumption did not notably affect the goodness-of-fit. Furthermore, Wang et al. (2022) calibrated the model by simulating customer and vehicle data in two hypothetical square regions (with  $p = 1, 2$ ) and one real-world region in New York City. The parameter values obtained from the two hypothetical square regions are similar to each other (i.e., the value of  $p$  did not make any major difference), but those from the New York City case differ notably.

Table 1: Parameter Values in the Literature.

Model Type and Study		Region	$m, n$	$\alpha_0$	$\alpha_1$	$\alpha_2$	
Assumed	Yang and Yang (2011)	-	-	0.2	0.75	0.75	
				10	0.5	0.5	
				200	0.25	0.25	
	Zha et al. (2016)	-	-	(0, 3]	0.6	0.6	
					0.7	0.7	
0.8					0.8		
Regression (empirical data)	Yang et al. (2014)	Hong Kong	-	0.0177	0.4080	0.7550	
	Zhang et al. (2019)	Shenzhen	-	13.3875	0.4569	0.4569	
				1.2011	0.2052	0.6760	
Regression (simulated data)	Wang et al. (2022)	Square, $p = 1$	-	4.2083	0.5274	0.5270	
		Square, $p = 2$		4.1950	0.5246	0.5260	
		New York City		7.2849	0.3877	0.4077	
Conjecture	Zha et al. (2016)	-	$m \ll n$	-	1	-	
Theoretical	Daganzo (1978)	Quasi-circle, $p = 1$	$1 = m \ll n$	$2\sqrt{2/\pi}$	1	0.5	
		Quasi-circle, $p = 2$		2	1	0.5	
	Equation (15)	Hyper-ball	$1 = m \ll n$	$1/\Gamma(\frac{3}{2})R(2, p)$	1	0.5	
	Equation (21)	Hyper-ball	$1 < m \ll n$	$1/R(2, p)$	1	0.5	
	Equation (11)	Hyper-ball	$\forall m, n$	-	-	-	

These studies presented very interesting findings (e.g., showing that the parameter values should depend on the region’s characteristics), but did not reveal any clear quantitative relationships. More importantly, it is not clear whether the Cobb-Douglas form is universally applicable to all settings (e.g., region shape, size, distance metric, dimensions, and  $m$  versus  $n$  values). Regarding the latter, Wei et al. (2022) conducted a large set of regression analyses to compare the model predictions with simulation outcomes under 420 different settings. It was found that the parameters in the Cobb-Douglas function vary notably across these settings, and the Cobb-Douglas function might fit quite poorly in certain settings (e.g., when  $n$  is small).

Zha et al. (2016) also argued (without theoretical proof) that one may simply set  $\alpha_1 = 1$  when the number of idle vehicles far exceeds the number of customers (i.e.,  $m \ll n$ ). This might be inspired by the intuition that when  $m$  is small, the customer waiting time should be solely dependent on the number of vehicles  $n$ . The only known theoretical result, derived first in Daganzo (1978) and later in Arnott (1996), states that for the special case of  $1 = m \ll n$ , the customer waiting time can be expressed in the form of Equation (22) with  $\alpha_0 = 2\sqrt{2/\pi}$  (when  $p = 1$ ) or 2 (when  $p = 2$ ),  $\alpha_1 = 1$  and  $\alpha_2 = 0.5$ . However, no theoretical proof was provided for the more general case when  $m \neq 1$ .

Next we show how our results in Sections 3 and 4 can be used to reveal (i) conditions under which the Cobb-Douglas meeting function Equation (22) can be applied, and under such conditions, (ii) the closed-form formulas for the values of parameters  $\alpha_0$ ,  $\alpha_1$  and  $\alpha_2$ . For taxi services, we set  $D = 2$  and use proper  $du$  and  $tu$  so that the value of customer waiting time is simply given

by  $E[X]$ . For the simplest case when  $1 = m \ll n$ , Equation (15) gives the customer waiting time  $E_1[X] = \Gamma(\frac{3}{2})R(2, p)/n^{\frac{1}{2}}$ , indicating that  $\alpha_0, \alpha_1$  and  $\alpha_2$  should take values  $1/\Gamma(\frac{3}{2})R(2, p)$ , 1 and 0.5, respectively. Such a result is clearly consistent with, but generalizes, the result in Daganzo (1978) with any  $L^p$  metric. When  $1 < m \ll n$ , setting  $\kappa \geq 1$  in Equation (15) no longer provides us with a Cobb-Douglas form formula. However, if we use  $\kappa = 0$ , the simplest asymptotic formula in Equation (21) can be employed and the customer waiting time approximately equals  $\hat{E}_0 = R(2, p)/n^{\frac{1}{2}}$ . This indicates that  $\alpha_0, \alpha_1$  and  $\alpha_2$  can now take values  $1/R(2, p)$ , 1 and 0.5, respectively. These are summarized in the last few rows of Table 1.

It is important to note that Equation (21) only provides an asymptotic approximation when  $1 < m \ll n$ . Hence, the Cobb-Douglas meeting function may be suitable only in a similar setting. For a more accurate estimations, especially in cases with more general combinations of  $n$  and  $m$ , we should refrain from using the simple Cobb-Douglas function. Instead, the general formula Equation (11) shall be used for these cases.

### 5.2. Optimal demand pooling for ride sharing

Next, we show how our formulas can be used to optimize e-hailing service strategies. Consider a 2-dimensional service region (i.e.,  $D = 2$ ) with an area size of 1 [ $\text{du}^2$ ], served by vehicles traveling at an average speed of 1 [ $\text{du}/\text{tu}$ ]. Customer trips are generated from a spatiotemporally homogeneous Poisson process, with rate  $\lambda$  [trips/ $\text{du}^2\text{-tu}$ ], such that each trip's origin and destination are uniformly distributed in the region. The vehicles in the system may transition among three states: idle, assigned, and in-service. An idle vehicle, upon assignment to a customer, will start a deadheading trip from its current location to the customer's origin, while at the same time, the customer starts to wait for pickup. After reaching the customer's origin, the vehicle becomes in-service and starts to move towards the customer's destination. When the in-service vehicle drops off the customer, it becomes idle again.

The service platform periodically matches and assigns idle vehicles to the customers at a set of discrete decision epochs. Between any two consecutive epochs, the newly idle vehicles and newly arriving customers are accumulated into their respective pools. At the latter decision epoch, an RBMP instance is solved to match all those customers and vehicles in these pools. The average optimal matching distance per customer-vehicle pair, with an expectation of  $E[X]$ , is the expected deadheading distance to pick up a customer.

While the system might be time-varying, we focus on a specific decision epoch, and denote the length of the corresponding pooling interval as  $\tau$ . The value of  $\tau$  directly affects the numbers of accumulated customers and vehicles and in turn affects  $E[X]$ . Yet, it is also directly experienced as extra "waiting" or idle time of both the customers and the vehicles. Therefore, the ride sharing platform needs to identify the optimal  $\tau$  value that minimizes the overall system "waiting" time per customer, including that for vehicle deadheading,  $E[X]$ , and the average wait for pooling,  $\frac{\tau}{2}$ :

$$E[X] + \beta \cdot \frac{\tau}{2}. \quad (23)$$

Here  $\beta$  is a relative weight that should normally be larger than 1; e.g., to account for the customer anxiety before a vehicle is assigned, and the fact that we assume there are more idle vehicles than customers at each matching epoch.

Next, two types of systems with different vehicle arrival dynamics are analyzed: one is an "open-loop" system without vehicle conservation, possibly representing services with freelance drivers; the



other is a “closed-loop” system with conservation of a fixed fleet of vehicles, possibly representing services with full-time drivers or robo-taxis.

### 5.2.1. Open-loop system

In the open-loop system that we consider, new idle vehicles arrive from outside of the system according to an independent process, and their initial locations are uniformly distributed in the region. This mimics a service scenario discussed in Yang et al. (2020), where the total fleet size in the system, as well as the numbers of vehicles in the three states, changes over time. Let  $n_i$  denote the number of idle vehicles in the system right after a previous decision epoch, and let  $\lambda'$  [trips/du<sup>2</sup>-tu] denote the expected arrival rate of idle vehicles (including those transitioned from the in-service state, and those new arrivals from outside). Right before the next decision epoch, the expected number of waiting customers in the pool is  $\lambda\tau$ , and the expected number of idle vehicles is  $n_i + \lambda'\tau$ . Hence, from our general formula (11), we know that  $E[X]$  is solely dependent on  $\tau$ , as

$$m = \lambda\tau, \quad n = n_i + \lambda'\tau. \quad (24)$$

Then, we can write a simple optimization model to minimize (23), as follows.

$$\begin{aligned} \min_{\tau} \quad & (23) \\ \text{s.t.} \quad & (11) \text{ and } (24), \\ & \tau \geq \frac{1}{\lambda}. \end{aligned} \quad (25)$$

Here Equation (11) can also be replaced by any of the formulas in Section 4. Constraint (25) specifies a boundary condition that at least one customer arrives during the pooling interval.

This optimization problem takes  $\lambda$ ,  $\lambda'$  and  $n_i$  as input and involves only one decision variable  $\tau$ . Thus, it can be easily solved numerically (without simulations). Furthermore, we can obtain some qualitative insights from the analytical formulation. Note the following: (i) from Equation (24),  $m$  and  $n$  both monotonically increase with  $\tau$ ; (ii) from the discussion in Section 3,  $E[X]$  decreases monotonically with  $n$  and increases monotonically with  $m$ . Hence, it is possible for  $E[X]$ , as well as Equation (23), to either increase or decrease with  $\tau$ . Two representative scenarios may arise here: (i) the objective function (23) monotonically increases with  $\tau$  and the optimal solution is simply  $\tau^* = \frac{1}{\lambda}$ , which implies that instantly matching each customer upon its arrival (i.e., “instant matching” as in Daganzo and Ouyang (2019); Ouyang and Yang (2023); Shen and Ouyang (2023)) might be a (near-) optimal strategy; or (ii) the objective function (23) is a non-monotonic function of  $\tau$ , such that the optimal solution  $\tau^* > \frac{1}{\lambda}$ , which indicates that pooling multiple customers into a batch for matching (i.e., “batch matching” as in Yang et al. (2020)) would be more favorable.

### 5.2.2. Closed-loop system

Now, we consider a closed-loop system which operates with a fixed fleet of  $S$  identical vehicles (i.e. no idle vehicles arrive from outside). Following the steady-state aspatial queuing network model in Daganzo (2010), we know that (i) the idle vehicle arrival rate equals the customer arrival rate; i.e.,

$$\lambda' = \lambda, \quad (26)$$

and (ii) the numbers of vehicles in the three states will reach a certain equilibrium (or jump between two equilibria). We denote the numbers of assigned and in-service vehicles right after the previous

decision epoch as  $n_a$  and  $n_s$ , respectively. They must satisfy vehicle conservation; i.e.,

$$S = n_i + n_s + n_a. \quad (27)$$

Let us further denote  $l$  [du] as the expected travel distance for an in-service vehicle to deliver a customer inside the unit-volume hyper-ball. Its value depends solely on the distance metric. Per Little's formula, in the steady state,  $n_s$  and  $n_a$  must also satisfy the following:

$$n_s = \lambda l, \quad n_a = \lambda \left( \mathbb{E}[X] + \frac{\tau}{2} \right). \quad (28)$$

Then, the optimization model in Section 5.2.1 can be adapted into the following:

$$\begin{aligned} \min_{\tau} \quad & (23), \\ \text{s.t.} \quad & (11) \text{ and } (24) - (28), \\ & 0 \leq n_i \leq S - \lambda\tau, \quad \lambda\tau \leq n_a \leq S, \quad 0 \leq n_s \leq S. \end{aligned} \quad (29)$$

Constraints (29) are boundary conditions that ensure the number of idle, assigned, or in-service vehicles, either before or after each decision epoch, cannot be negative nor exceed the fleet size.

This new optimization problem takes  $\lambda$  and  $S$  as input, but  $n_i$  now must be solved out of Equations (24), (26)-(28) for any  $\tau$ . Two roots of  $n_i$  may exist in correspondence to two equilibrium states of the system (Ouyang and Yang, 2023; Shen and Ouyang, 2023): the one with a larger  $n_i$  value is referred to as the efficient equilibrium; and the other with a smaller  $n_i$  value is referred to as the inefficient equilibrium (i.e., the so-called ‘‘wild goose chase (WGC)’’ phenomenon). The optimal value of  $\tau$  shall depend on the relative values of  $m$  and  $n$ , similar to the discussed cases in Section 5.2.1, around either equilibrium point.

## 6. Numerical Results

In this section, we present simulation results to verify the accuracy of the proposed distance formulas and also show case their applications to planning mobility services.

### 6.1. Verification of distance formulas

To verify the accuracy of the proposed distance formulas, a set of Monte-Carlo simulations are conducted, with which we generate 100 random instances of RBMP for each of the following parameter value combinations: space dimension  $D \in \{2, 3, 4, 5\}$ , distance metric parameter  $p \in \{1, 2\}$ , and various values of  $n$  and  $m$ . For each instance, the points' locations are spatially uniformly distributed in a unit-volume  $D$ -dimensional hyper-ball, and the instance is solved by a standard linear program solver Gurobi. The average of the optimal matching distances across the 100 instances is recorded as the sample mean of corresponding RBMP distance.

We first set  $D = 2$ ,  $p = 2$ ,  $m \in \{1, 10, 50, 200\}$ , and  $n$  ranging from  $m$  to a sufficiently large number. Figure 1 compares the Monte-Carlo simulation results with the following formulas:  $\mathbb{E}_{\kappa}[X]$  from Equation (15) (with  $\kappa \in \{0, 1, m\}$ );  $\hat{\mathbb{E}}_0[X]$  from Equation (18); and the simple asymptotic approximation of  $\hat{\mathbb{E}}_0[X]$  from Equation (21). The optimal matching distance from each simulated RBMP instance is represented by a light-blue dot, and their sample average is represented by the red solid line. The estimations from Equations (18), (21), and Equation (15) (with varying  $\kappa$

values) are represented by the dashed-dotted lines, the dotted lines, and the dashed lines (with varying colors), respectively.

Figure 1(a) shows results for the special case when  $m = 1$ . It can be observed that the estimations from all formulas closely match with the simulated sample averages. In particular, Equation (15) with  $\kappa = 1$  and  $\kappa = 0$  have an average relative error of 6.0% and 8.8%, respectively, across the entire range of  $n$  values. This suggests that setting  $\kappa = 0$  here (which is computationally appealing) does not sacrifice too much accuracy as compared to  $\kappa = 1$ . In addition, we note that when  $m = 1$ , Equation (18) equals Equation (21), and the average relative error for both is 8.8%. These results indicate that all the proposed formulas are providing a good estimate when  $m = 1$ .

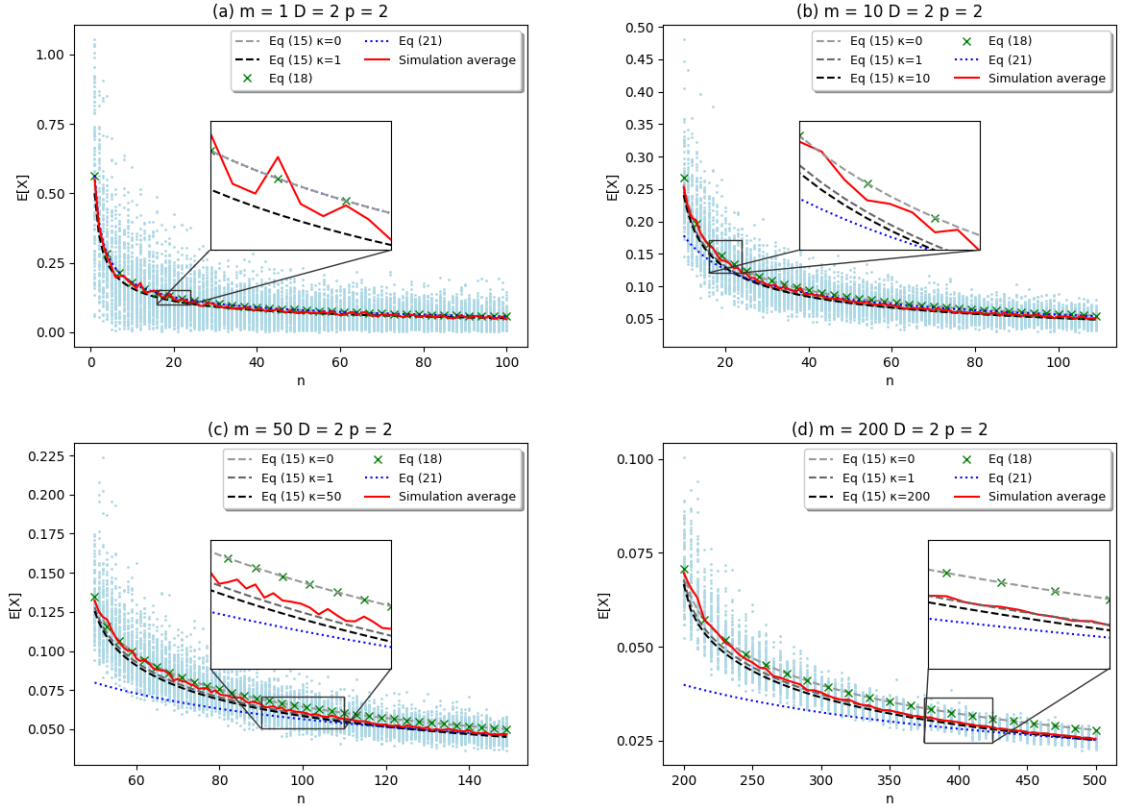


Figure 1: Accuracy of estimators under Euclidean distance.

When  $m > 1$ , Figures 1(b)-(d) show that the estimations from Equations (15) and (18) all match well with the simulated result across all the  $n$  values; the only exception is Equation (21), which yields larger gaps when  $n \approx m$ . When  $m = 50$ , as an example, the average relative errors of Equation (15) with  $\kappa = 0, 1, 50$  are 5.2%, 2.4%, 4.2% respectively, and that of Equation (18) is 5.2%. Similar patterns can also be seen for the other cases when  $m = 10$  and  $m = 200$ . If we take a closer look at the curves for Equation (15), little difference can be observed between those from  $\kappa = 1$  and  $\kappa = m$ , and they all align more closely with the simulated results as  $n \rightarrow \infty$ . This suggests that choosing  $\kappa = 0$  or 1 can already provide a sufficiently accurate estimation, as compared to the computationally more challenging choice of  $\kappa = m$ .

While the errors from Equation (21), as shown in Figure 1(b)-(d), are non-negligible when  $n \approx m$ , they quickly diminish as  $n$  increases. Figure 1 (a)-(d) show that the error becomes almost

the same as those of other formulas when  $n \geq 2m$ . This is consistent with Proposition 4, which says that Equation (21) is a suitable approximation only when  $n \gg m$ .

Next, we study the impacts of distance metrics. We now set  $D = 2$ ,  $p = 1$ . Figure 2 shows counterpart of Figure 1 with the same set of  $n$  and  $m$  combinations. As shown, Equations (15) and (18) again both match quite well with the simulated results across all  $m$  and  $n$  values. When  $m = 50$ , as an example, the average relative errors of Equation (15) with  $\kappa = 0, 1, 50$  are 6.4%, 2.3%, and 3.9% respectively, and that of Equation (18) is 6.4%. Again, it can be observed from the close-up plots in Figure 2(a)-(d) that when  $n \geq 2m$ , Equation (21) starts to provide very good estimations. All these observations are consistent with those seen from the previous case when  $p = 2$ . Recall from Section 3.2.3 that under different  $p$ ,  $E[X]$  varies only by a constant multiplicative factor  $R(D, p)$ . This is clearly confirmed by our numerical results here, where  $D = 2$ , because the ratios of all simulated and formula predictions of  $E[X]$  values in Figure 2 to their counterparts in Figure 1 are consistently around  $\frac{R(2,1)}{R(2,2)} = \frac{\sqrt{2\pi}}{2} \approx 1.253$ .

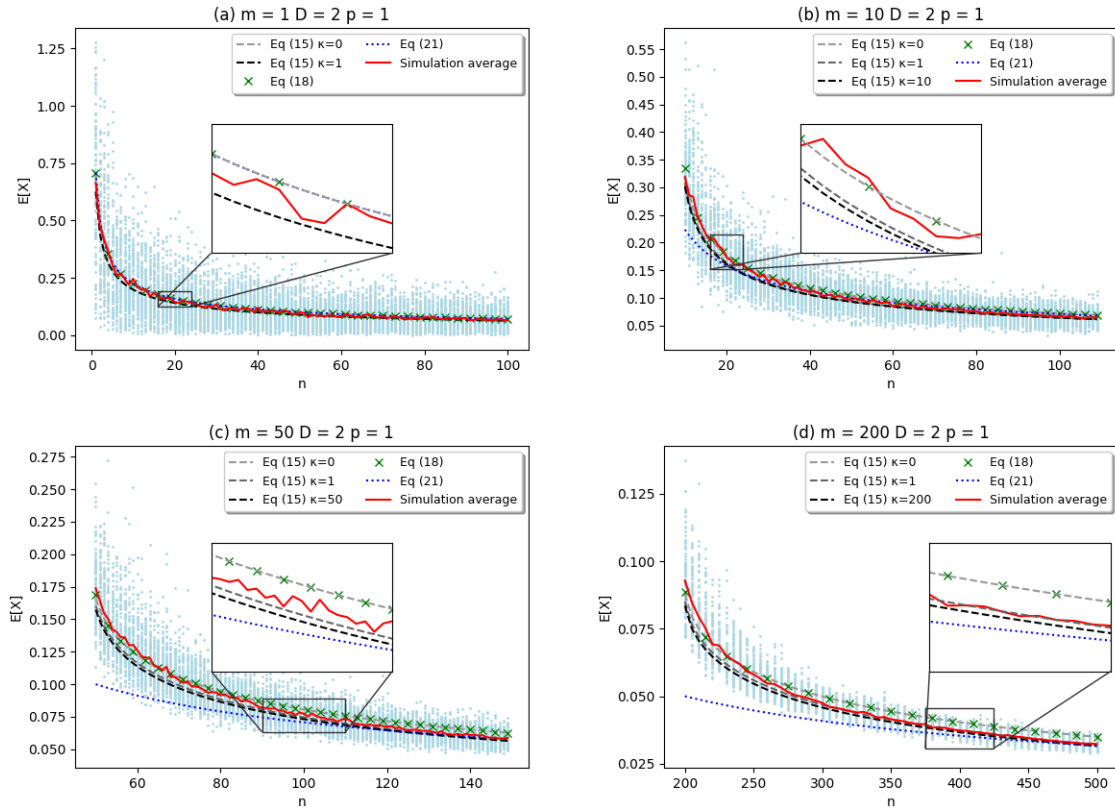


Figure 2: Distance estimators under Manhattan distance.

Finally, we study the impacts of dimension  $D$ . Now we set  $p = 2$  and  $D \in \{3, 4, 5\}$ , and plot in Figure 3 the results for the case when  $m = 50$ . Recall that the baseline case for  $D = 2$  is shown in Figure 1(c). When  $D = 3$ , all estimations from Equations (15) and (18) still align well with the simulated results, with errors in the range of about 5%. However, as  $D$  increases to 4 and 5, the error becomes somewhat larger for most formulas. Taking Equation (15) with  $\kappa = 50$  as an example, the average relative errors are 4.2%, 5.6%, and 7.0% for  $D = 3, 4$ , and  $5$  respectively. This pattern occurs because, in deriving the expected distance to one's  $k$ th nearest neighbor (i.e.,  $E[Y_k]$ )

in Section 3.2.2, we assume that the “generic” reference point is at the center of the hyper-ball. However, as the number of dimension increases, the ratio of the hyper-ball’s surface area to its volume increases, such that a random point would be more likely to be closer to the surface (farther away from the center). As a result, our estimate for  $E[Y_k]$ , and hence that for  $E[X]$ , become less accurate in higher dimensional spaces (e.g.,  $D \geq 4$ ). Fortunately, most real-world mobility systems involve a spatial dimension of  $D = 2$  and  $D = 3$ . This assures that the proposed formulas could be useful for service planning. This will be demonstrated in the next subsection.

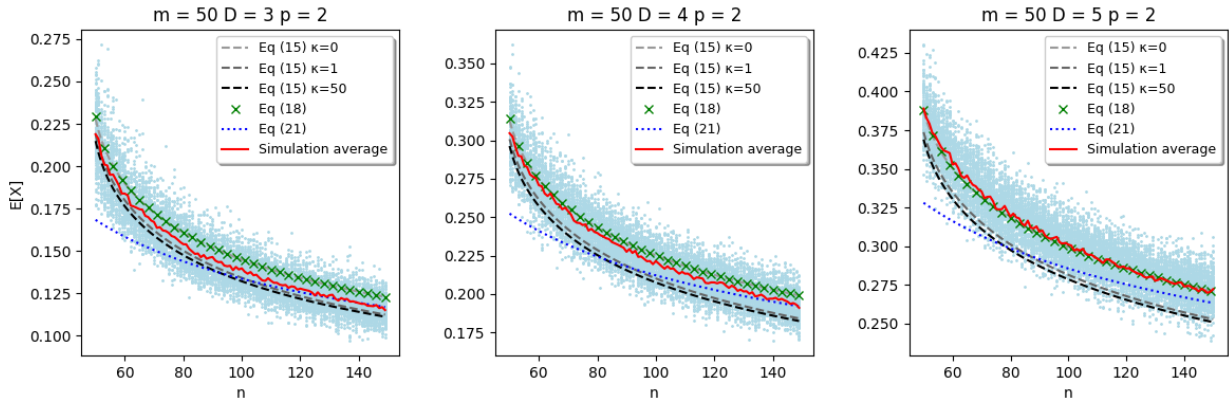


Figure 3: Distance estimator under different dimension.

## 6.2. Effectiveness of demand pooling

Two simulation programs are developed to verify the effectiveness of the demand pooling strategy for the open- and closed-loop e-hailing taxi systems in Section 5.2. A series of numerical experiments are conducted to compare simulation measurements with model results. In all experiments, we set  $p = 2$  and  $\beta = 1$ , and  $E[X]$  is estimated from Equation (15) with  $\kappa = 0$ .

The program for the open-loop system simulates the arrivals of customers and vehicles in a specific pooling interval before a decision epoch. At the beginning of each simulation (i.e., time 0),  $n_i$  idle vehicles are distributed uniformly within a unit-area circle. Then, customer trips and new idle vehicles are generated from two independent homogeneous spatio-temporal Poisson processes with rates  $\lambda$  and  $\lambda'$  [trips/du<sup>2</sup>-tu], respectively. We select a sample of  $\tau$  [tu] values. For each  $\tau$  value, we use commercial solver Gurobi to solve an RBMP instance with the accumulated customers and idle vehicles by time  $\tau$ , and each matched customer’s waiting times for pooling and for pickup are recorded.

Experiments are conducted under a set of parameter combinations:  $\lambda = \lambda' \in \{200, 500, 1000\}$ , and  $n_i \in \{10, 30, 100\}$ . We select 10 discrete  $\tau$  values that are evenly distributed between  $\frac{1}{\lambda}$  and 0.1 [tu]. For each parameter combination and  $\tau$  value, we run  $30/\tau$  simulations and take the average. The results are shown in Figure 4. Model estimations of Equation (23) for  $n_i \in \{10, 30, 100\}$  are represented by the red dashed curve, green dash-dot curve, and blue dotted curve, respectively. Meanwhile, the simulation measurements are represented by the red triangles, green cross markers, and blue plus markers, respectively. It can be observed that the objective value estimations, for all  $\tau$ , match quite well with their corresponding simulation averages. When demand is relatively lower,  $\lambda = \lambda' \in \{200, 500\}$  and there are abundant idle vehicles,  $n_i = 30$  and 100, as we can see from Figures 4(a)-(b), the value of Equation (23) monotonically increases with  $\tau$ , and hence  $\tau^* = \frac{1}{\lambda}$ .

This corresponds to the case of scenario (i) as discussed in Section 5.2.1, where “instant matching” is more favorable. However, when the number of idle vehicles is smaller,  $n_i = 10$ , Equation (23) first decreases and then increases with  $\tau$ , such that notably  $\tau^* > \frac{1}{\lambda}$ . This corresponds to the case of scenario (ii) where “batch matching” is more favorable. Also, when demand increases to  $\lambda = \lambda' = 1000$ , as shown in Figure 4(c), it is more likely for batch matching to be favorable for  $n_i = 10$  and 30. These observations are consistent with our analytical insights in Section 5.2, and suggest that: the simpler instant matching strategy might be very suitable when the taxi system has a sufficient number of idle vehicles and it does not expect a large number of new idle vehicles arriving from outside of the system; meanwhile, batch matching is likely to be beneficial when the system is about to run out of idle vehicles, or if it expects a large number of new idle vehicles to arrive from outside.

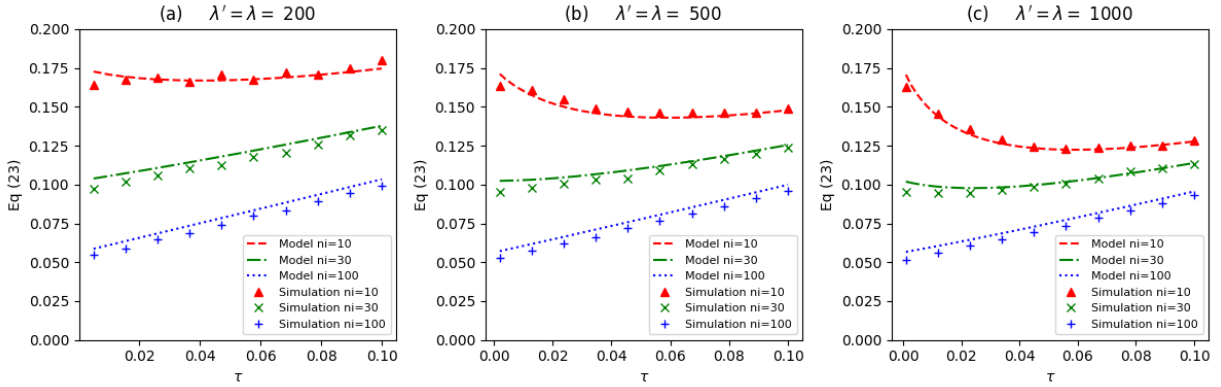


Figure 4: Estimated vs. simulated Eq (23) of an open-loop system under different  $\lambda$  and  $n_i$ .

For the closed-loop system, an agent-based simulation program is developed. It tracks each customer’s and vehicle’s entire travel experience, including arrival, assignment, pickup and drop-off. The program generates customer trips from a Poisson process with rate  $\lambda$  [trips/du<sup>2</sup>-tu], similar to that for the open-loop system, but now a fixed fleet of  $S$  vehicles are used to serve these trips. The customers and vehicles evolve following the processes described in Section 5.2, and bipartite matching between waiting customers and idle vehicles is conducted at times  $\tau, 2\tau, \dots$  [tu]. Any unmatched customers (e.g., due to random demand surges) are removed from the system and considered as lost.

Experiments are conducted under a set of parameter combinations. We use the same  $\lambda$  and  $\tau$  values as those for the open-loop system. We can compute the minimum required fleet size to serve all customers in a steady state (Daganzo, 2010), which are approximately 143, 330, and 630 for  $\lambda \in \{200, 500, 1000\}$ , respectively. Based on this information, we try two fleet sizes to represent smaller and large fleet scenarios: the values of  $S \in \{155, 220\}, \{360, 500\}$  and  $\{680, 1000\}$ , respectively. For each parameter combination, one simulation run with a duration of 30 [tu] is performed. The first 6 [tu] of each simulation run is considered as the warm-up period, and we only record data from the later part. The corresponding model estimations are computed based on Equations (23)-(24) and (26)-(28).

The results are shown in Figure 5. Model estimations are represented by the red dashed curve and blue dash-dot curve, respectively, for the small and large  $S$  values. The corresponding simulation averages are represented by the red cross markers and blue plus markers, respectively.

When  $S$  is sufficiently large, only one blue dash-dot curve appears in each sub-figure, indicating the system has only one (efficient) equilibrium state (Ouyang and Yang, 2023). In this case, Equation (23) monotonically increases with  $\tau$ , which falls into the case of scenario (i), and the simulation averages across all demand levels match well with the model estimations (as shown in Figure 5(a)-(c)). When  $S$  is relatively small, two red dashed curves appear in each sub-figure, indicating the system can potentially have both inefficient and efficient equilibrium states. It can also be seen that the upper red dashed curve is truncated as  $\tau$  increases beyond a certain threshold, which indicates that the inefficient equilibrium (WGC) may completely disappear if demand is pooled for a sufficiently long time period — a significant potential benefit of demand pooling. Yet, if we only focus on only the efficient equilibrium, we shall still do instant matching because Equation (23) for the efficient equilibrium monotonically increases with  $\tau$ .

In addition, we shall note that when two equilibrium states exist, the simulation measurements may be the average of the two equilibrium points (weighted by the duration the system spends in either equilibrium); see more discussion in (Ouyang and Yang, 2023). Yet, most of these simulation measurements still align well with the model estimations (especially when the fleet size is large) for the efficient equilibrium — implying that the system predominantly stay in the efficient equilibrium state under those conditions. All these observations imply that, in a closed-loop system, instant matching might again be an effective strategy overall. Batch matching may only be beneficial for counteracting the WGC phenomenon when the system with a small fleet size is currently stuck in an inefficient equilibrium state.

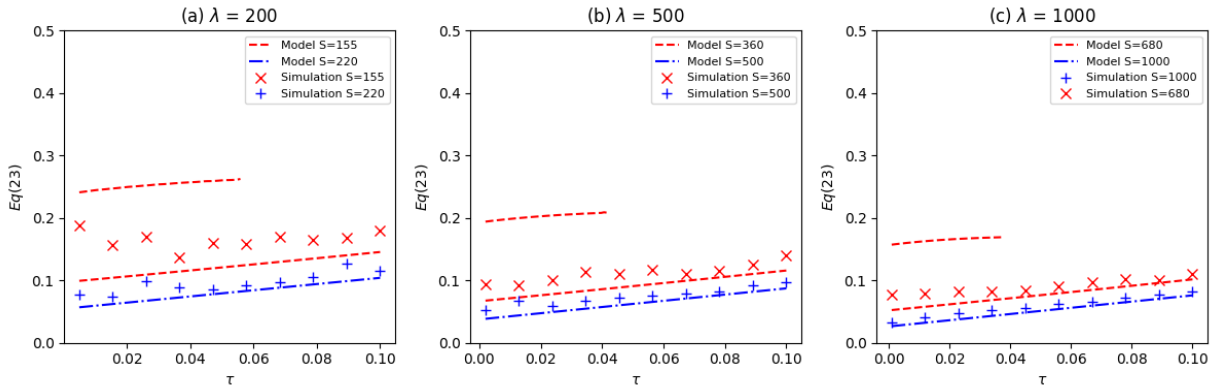


Figure 5: Estimated vs. simulated Eq (23) of a closed-loop system under different  $\lambda$  and  $S$ .

## 7. Conclusion

This paper proposes analytical closed-form formulas (without statistical curve-fitting) that estimate the probability distribution and expectation of the optimal matching distance from a random bipartite matching problem (RBMP) in a  $D$ -dimensional  $L^p$  space. Asymptotic approximations of the formulas (with varying levels accuracy and computation complexity) are also derived for special problem settings (such as the relative numbers of bipartite vertices) — as such, one can select the most suitable formula based on the specific problem setting and the need for formula accuracy. Through a series of Monte-Carlo simulation experiments, our formulas are shown to be

able to provide accurate RBMP distance estimations under a variety of conditions (e.g., regarding the numbers of bipartite vertices, spatial dimensions, and distance metrics).

Using mobility services as an example, this paper shows how the proposed formulas can be used to provide managerial insights on the expected matches between randomly distributed customers and service vehicles. For instance, the formulas confirm that distance metric impacts the expected optimal matching distance only by a constant multiplicative factor. In addition, the formulas also provide a theoretical explanation on when and why the empirically assumed Cobb-Douglas matching functions are suitable for mobility systems. The proposed distance formulas are also particularly useful for strategic planning or allocation of resources in mobility services. For example, this paper shows how they can be integrated into optimization models to plan e-hailing taxi operational strategies (e.g., choosing demand pooling intervals) under two system settings. The predicted performance of these strategies are verified by agent-based simulations. The results not only show that the model estimates match quite well with the simulation measurements under all tested service settings, but also provide insights on suitability of instant matching vs. batch matching strategies: instant matching is more favorable when the system has a sufficiently large fleet, while batch matching can be beneficial when the system with a small fleet (e.g., to avoid the inefficient equilibrium).

The current modeling approach builds upon several simplifying assumptions that could be relaxed in the future. In Section 3, we assume that (i) all vertices within each subset are identically and independently distributed over space, (ii) the impacts of spatial boundaries are negligible, and (iii) the matches among the vertices are made independently of one another. These assumptions have two impacts on the accuracy of our formulas. First, assumptions (i) and (ii) imply that the “generic” reference vertex analyzed in Section 3.2.2 could be regarded as being at the “center” of the hyper-ball. As discussed in Section 6.1, this does not significantly impact the estimates for  $E[X]$  when  $D = 2$  or  $D = 3$ . However, the estimates may become less accurate when  $D$  increases, because in these higher dimensions a randomly distributed vertex is less likely to be near the center of the hyper-ball. Second, these assumptions ignore the correlation among vertex distributions and matchings in a bounded hyper-ball. As discussed in Section 3.1, the impacts of such correlations remain relatively small for  $D > 1$ , but will become significant when  $D = 1$ . Future research should attempt to relax all these simplifying assumptions and explicitly consider the correlations among vertex distribution, matching, and impacts of the hyper-ball boundary. While this is a non-trivial task, the special case with  $D = 1$  is being investigated in a working paper (Zhai et al., 2024).

The proposed model and formulas could also be further extended to other problem settings or application contexts. First, more accurate asymptotic approximations for certain special cases (such as when  $m \approx n \gg 1$ ) hold the promise for providing more theoretical and practical connections to those in the field of statistical physics (e.g., those in Caracciolo et al. (2014)) for the balanced case (i.e.,  $m = n$ ). It would be interesting to see if insights and theoretical justifications (similar to those in Section 5.1) could be found for those results. Second, it will be interesting to extend the model as building blocks for other problems. For example, the current RBMP is defined as a static problem, and the matching decisions are made with full knowledge of all point locations. It can be generalized into a dynamic matching problem where matching decisions must be made based on incomplete information on future point arrivals. As discussed in Section 2, Kanoria (2022) showed, by adopting a hierarchical greedy algorithm, how the bounds to the expected matching distance for a static problem can be adapted into bounds of minimum achievable matching distance in a dynamic problem. Now that we have formulas to estimate the exact matching distance rather



than the bounds, it would be interesting to generalize our model to directly predict the expected matching distance in such a dynamic setting.

## Acknowledgments

This research was supported in part by the US DOT Region V University Transportation Center, and the ZJU-UIUC Joint Research Center Project No. DREMES-202001, funded by Zhejiang University.

## References

- Ajtai, M., Komlós, J., and Tusnády, G. (1984). On optimal matchings. *Combinatorica*, 4(4):259–264.
- Alm, S. E. and Sorkin, G. B. (2002). Exact Expectations and Distributions for the Random Assignment Problem. *Combinatorics, Probability and Computing*, 11(3):217–248.
- Ambrosio, L., Goldman, M., and Trevisan, D. (2021). On the quadratic random matching problem in two-dimensional domains. arXiv:2110.14372.
- Arnott, R. (1996). Taxi Travel Should Be Subsidized. *Journal of Urban Economics*, 40(3):316–333.
- Asratian, A. S., Denley, T. M. J., and Häggkvist, R. (1998). *Bipartite Graphs and their Applications*. Cambridge Tracts in Mathematics. Cambridge University Press, Cambridge.
- Bhattacharyya, P. and Chakrabarti, B. K. (2008). The mean distance to the  $n$  th neighbour in a uniform distribution of random points: an application of probability theory. *European Journal of Physics*, 29(3):639–645.
- Boas Jr., R. P. and Wrench Jr., J. W. (1971). Partial Sums of the Harmonic Series. *The American Mathematical Monthly*, 78(8):864–870.
- Boniolo, E., Caracciolo, S., and Sportiello, A. (2014). Correlation function for the Grid-Poisson Euclidean matching on a line and on a circle. *Journal of Statistical Mechanics: Theory and Experiment*, 2014(11):P11023.
- Brunetti, R., Krauth, W., Mézard, M., and Parisi, G. (1991). Extensive Numerical Simulations of Weighted Matchings: Total Length and Distribution of Links in the Optimal Solution. *Europhysics Letters (EPL)*, 14(4):295–301.
- Caracciolo, S., Lucibello, C., Parisi, G., and Sicuro, G. (2014). Scaling hypothesis for the Euclidean bipartite matching problem. *Physical Review E*, 90(1):012118.
- Caracciolo, S. and Sicuro, G. (2014). One-dimensional Euclidean matching problem: Exact solutions, correlation functions, and universality. *Physical Review E*, 90(4):042112.
- Caracciolo, S. and Sicuro, G. (2015). Quadratic stochastic Euclidean bipartite matching problem. *Physical Review Letters*, 115(23):230601.
- Coppersmith, D. and Sorkin, G. B. (1998). Constructive Bounds and Exact Expectations for the Random Assignment Problem. In Luby, M., Rolim, J. D. P., and Serna, M., editors, *Randomization and Approximation Techniques in Computer Science*, pages 319–330, Berlin, Heidelberg. Springer.
- Daganzo, C. F. (1978). An approximate analytic model of many-to-many demand responsive transportation systems. *Transportation Research*, 12(5):325–333.
- Daganzo, C. F. (2010). *Public Transportation Systems: Basic Principles of System Design, Operations Planning and Real-Time Control*.
- Daganzo, C. F. and Ouyang, Y. (2019). A general model of demand-responsive transportation services: From taxi to ridesharing to dial-a-ride. *Transportation Research Part B: Methodological*, 126:213–224.
- Daganzo, C. F., Ouyang, Y., and Yang, H. (2020). Analysis of ride-sharing with service time and detour guarantees. *Transportation Research Part B: Methodological*, 140:130–150.
- Daganzo, C. F. and Smilowitz, K. R. (2004). Bounds and Approximations for the Transportation Problem of Linear Programming and Other Scalable Network Problems. *Transportation Science*, 38(3):343–356.
- Jonker, R. and Volgenant, A. (1987). A shortest augmenting path algorithm for dense and sparse linear assignment problems. *Computing*, 38(4):325–340.
- Jowett, G. H. (1963). The Relationship Between the Binomial and F Distributions. *Journal of the Royal Statistical Society. Series D (The Statistician)*, 13(1):55–57.
- Kanoria, Y. (2022). Dynamic Spatial Matching. In *Proceedings of the 23rd ACM Conference on Economics and Computation*, pages 63–64, Boulder CO USA. ACM.
- Kershaw, D. (1983). Some Extensions of W. Gautschi’s Inequalities for the Gamma Function. *Mathematics of Computation*, 41(164):607–611. Publisher: American Mathematical Society.

- Kuhn, H. W. (1955). The Hungarian method for the assignment problem. *Naval Research Logistics Quarterly*, 2(1-2):83–97.
- Lei, C. and Ouyang, Y. (2024). Average minimum distance to visit a subset of random points in a compact region. *Transportation Research Part B: Methodological*, 181:102904.
- Linusson, S. and Wästlund, J. (2004). A proof of Parisi’s conjecture on the random assignment problem. *Probability Theory and Related Fields*, 128(3):419–440.
- Liu, Y. and Ouyang, Y. (2021). Mobility service design via joint optimization of transit networks and demand-responsive services. *Transportation Research Part B: Methodological*, 151:22–41.
- Liu, Y. and Ouyang, Y. (2023). Planning ride-pooling services with detour restrictions for spatially heterogeneous demand: A multi-zone queuing network approach. *Transportation Research Part B: Methodological*, 174:102779.
- Mézard, M. and Parisi, G. (1985). Replicas and optimization. *Journal de Physique Lettres*, 46(17):771–778.
- Mézard, M. and Parisi, G. (1988). The Euclidean matching problem. *Journal de Physique*, 49(12):2019–2025.
- Nair, C., Prabhakar, B., and Sharma, M. (2005). Proofs of the Parisi and Coppersmith-Sorkin random assignment conjectures. *Random Structures & Algorithms*, 27(4):413–444.
- Olver, F. W. (2010). *NIST handbook of mathematical functions hardback and CD-ROM*. Cambridge university press.
- Ouyang, Y. and Yang, H. (2023). Measurement and mitigation of the “wild goose chase” phenomenon in taxi services. *Transportation Research Part B: Methodological*, 167:217–234.
- Ouyang, Y., Yang, H., and Daganzo, C. F. (2021). Performance of reservation-based carpooling services under detour and waiting time restrictions. *Transportation Research Part B: Methodological*, 150:370–385.
- Parisi, G. (1998). A Conjecture on random bipartite matching. arXiv:cond-mat/9801176.
- Shen, S. and Ouyang, Y. (2023). Dynamic and Pareto-improving swapping of vehicles to enhance integrated and modular mobility services. *Transportation Research Part C: Emerging Technologies*, 157:104366.
- Simmons, B. I., Cirtwill, A. R., Baker, N. J., Wauchope, H. S., Dicks, L. V., Stouffer, D. B., and Sutherland, W. J. (2019). Motifs in bipartite ecological networks: uncovering indirect interactions. *Oikos*, 128(2):154–170.
- Talagrand, M. (1992). Matching Random Samples in Many Dimensions. *The Annals of Applied Probability*, 2(4):846–856. Publisher: Institute of Mathematical Statistics.
- Tanay, A., Sharan, R., Kupiec, M., and Shamir, R. (2004). Revealing modularity and organization in the yeast molecular network by integrated analysis of highly heterogeneous genomewide data. *Proceedings of the National Academy of Sciences*, 101(9):2981–2986.
- Wang, G., Zhang, H., and Zhang, J. (2022). On-Demand Ride-Matching in a Spatial Model with Abandonment and Cancellation. *Operations Research*.
- Wei, S., Feng, S., Ke, J., and Yang, H. (2022). Calibration and validation of matching functions for ride-sourcing markets. *Communications in Transportation Research*, 2:100058.
- Wood, D. (1992). The computation of polylogarithms. Technical Report 15-92\*, University of Kent, Computing Laboratory, University of Kent, Canterbury, UK.
- Wu, S., Sun, F., Zhang, W., Xie, X., and Cui, B. (2022). Graph Neural Networks in Recommender Systems: A Survey. *ACM Computing Surveys*, 55(5):97:1–97:37.
- Yang, H., Leung, C. W., Wong, S., and Bell, M. G. (2010). Equilibria of bilateral taxi–customer searching and meeting on networks. *Transportation Research Part B: Methodological*, 44(8-9):1067–1083.
- Yang, H., Qin, X., Ke, J., and Ye, J. (2020). Optimizing matching time interval and matching radius in on-demand ride-sourcing markets. *Transportation Research Part B: Methodological*, 131:84–105.
- Yang, H. and Yang, T. (2011). Equilibrium properties of taxi markets with search frictions. *Transportation Research Part B: Methodological*, 45(4):696–713.
- Yang, T., Yang, H., Wong, S. C., and Sze, N. N. (2014). Returns to scale in the production of taxi services: an empirical analysis. *Transportmetrica A: Transport Science*, 10(9):775–790.
- Yu, H., Ye, W., Feng, Y., Bao, H., and Zhang, G. (2020). Learning Bipartite Graph Matching for Robust Visual Localization. In *2020 IEEE International Symposium on Mixed and Augmented Reality (ISMAR)*, pages 146–155, Porto de Galinhas, Brazil. IEEE.
- Zha, L., Yin, Y., and Yang, H. (2016). Economic analysis of ride-sourcing markets. *Transportation Research Part C: Emerging Technologies*, 71:249–266.
- Zhai, Y., Shen, S., and Ouyang, Y. (2024). Exact formula for estimating the average optimal distance in one-dimensional bipartite matching problem. Working Paper. University of Illinois at Urbana-Champaign.
- Zhang, J., Liu, C., Li, X., Zhen, H.-L., Yuan, M., Li, Y., and Yan, J. (2023). A survey for solving mixed integer programming via machine learning. *Neurocomputing*, 519:205–217.
- Zhang, K., Chen, H., Yao, S., Xu, L., Ge, J., Liu, X., and Nie, M. (2019). An Efficiency Paradox of Uberization. *SSRN Electronic Journal*.

Zhou, T., Ren, J., Medo, M., and Zhang, Y. (2007). Bipartite network projection and personal recommendation. *Physical Review E*, 76(4):046115.

### Appendix A. Proof for Lemma 3

**Lemma 3.** For  $z \in \mathbb{Z}^+, D \in \mathbb{Z}^+$ ,

$$0 \leq z^{\frac{1}{D}} - \frac{\Gamma(z + \frac{1}{D})}{\Gamma(z)} < 1 - \frac{\sqrt{3}}{2}.$$

*Proof.* For the trivial case when  $D = 1$ ,  $\frac{\Gamma(z+1)}{\Gamma(z)} = z$  and the inequalities clearly hold. We now consider the case when  $D \geq 2$ . Kershaw (1983) showed that for any  $x > 0$  and  $0 < s < 1$ , the following must hold:

$$\left(x + \frac{s}{2}\right)^{1-s} < \frac{\Gamma(x+1)}{\Gamma(x+s)} < \left[x - \frac{1}{2} + \left(s + \frac{1}{4}\right)^{\frac{1}{2}}\right]^{1-s}.$$

Since  $z \in \mathbb{Z}^+, D \in \mathbb{Z}^+$ , we can let  $x = z - s > 0$  and  $0 < s = 1 - \frac{1}{D} < 1$ , and as such:

$$\left(z - \frac{1 - \frac{1}{D}}{2}\right)^{\frac{1}{D}} < \frac{\Gamma(z + \frac{1}{D})}{\Gamma(z)} < \left[z - \left(\frac{3}{2} - \frac{1}{D}\right) + \left(\frac{5}{4} - \frac{1}{D}\right)^{\frac{1}{2}}\right]^{\frac{1}{D}}. \quad (\text{A.1})$$

When  $D \geq 2, z \in \mathbb{Z}^+$ , simple algebra shows that the right hand side of (A.1) is strictly less than  $z^{\frac{1}{D}}$ , and therefore  $z^{\frac{1}{D}} - \frac{\Gamma(z + \frac{1}{D})}{\Gamma(z)} > 0$ .

Meanwhile, the left hand side of (A.1) leads to  $z^{\frac{1}{D}} - \frac{\Gamma(z + \frac{1}{D})}{\Gamma(z)} < z^{\frac{1}{D}} - \left(z - \frac{1 - \frac{1}{D}}{2}\right)^{\frac{1}{D}}$ . Let  $\delta(z, D) = z^{\frac{1}{D}} - \left(z - \frac{1 - \frac{1}{D}}{2}\right)^{\frac{1}{D}}$ . It is easy to show that  $\frac{\partial \delta(z, D)}{\partial z} < 0$  for all  $z \in \mathbb{Z}^+, D \in \mathbb{Z}^+$ , and hence  $\delta(z, D)$  should monotonically decrease with  $z$  for any  $D$ ; i.e.,  $\delta(z, D) \leq \delta(1, D) = 1 - \left(\frac{1 + \frac{1}{D}}{2}\right)^{\frac{1}{D}}$ . For  $D \in \mathbb{Z}^+$ , this upper bound should take its maximum value  $1 - \frac{\sqrt{3}}{2}$  at  $D = 2$ . Therefore,  $z^{\frac{1}{D}} - \frac{\Gamma(z + \frac{1}{D})}{\Gamma(z)} < 1 - \frac{\sqrt{3}}{2}$ . This completes the proof.  $\square$

### Appendix B. Proof for Proposition 2

**Proposition 2.** When  $n \gg 1, \kappa \in \{0, \dots, m\}$ ,

$$0 \leq E_{\kappa}[X] - E[X] \leq \left(1 - \frac{\sqrt{3}}{2}\right) R(D, p) \cdot n^{-\frac{1}{D}},$$

and  $\lim_{n \rightarrow +\infty} (E_{\kappa}[X] - E[X]) \rightarrow 0$  for  $D < \infty$ .

*Proof.* Note from Lemma 3 that the approximation error to the gamma functions is always non-negative, and hence, for any  $\kappa_1 \leq \kappa_2 \in \{0, \dots, m\}$ , the following must hold:

$$E_{\kappa_1}[X] \geq E_{\kappa_2}[X] \geq E[X].$$

To show  $E_\kappa[X] - E[X] \leq \left(1 - \frac{\sqrt{3}}{2}\right) \frac{R(D,p)}{n^{\frac{1}{D}}}$  for all  $\kappa \in \{0, \dots, m\}$ , it suffices to show it for the extreme case when  $\kappa = 0$ :

$$\begin{aligned} E_0[X] - E[X] &= \frac{R(D,p)}{mn^{\frac{1}{D}}} \sum_{i=1}^m \sum_{k=1}^i \left[ \left(\frac{i-1}{n}\right)^{k-1} \left(1 - \frac{i-1}{n}\right) \left(k^{\frac{1}{D}} - \frac{\Gamma(k + \frac{1}{D})}{\Gamma(k)}\right) \right. \\ &\quad \left. + \left(\frac{i-1}{n}\right)^i \left(i^{\frac{1}{D}} - \frac{\Gamma(i + \frac{1}{D})}{\Gamma(i)}\right) \right] < \left(1 - \frac{\sqrt{3}}{2}\right) \frac{R(D,p)}{n^{\frac{1}{D}}}. \end{aligned}$$

Note the inequality holds because  $\frac{1}{m} \sum_{i=1}^m \sum_{k=1}^i \left[ \left(\frac{i-1}{n}\right)^{k-1} \left(1 - \frac{i-1}{n}\right) + \left(\frac{i-1}{n}\right)^i \right] = 1$ , and both  $\left(k^{\frac{1}{D}} - \frac{\Gamma(k + \frac{1}{D})}{\Gamma(k)}\right)$  and  $\left(i^{\frac{1}{D}} - \frac{\Gamma(i + \frac{1}{D})}{\Gamma(i)}\right)$  are less than  $1 - \frac{\sqrt{3}}{2}$  from Equation (14).

Obviously, for any finite value of  $D$ , the right hand side of the above inequality approaches 0 as  $n$  goes to infinity, and as such  $\lim_{n \rightarrow +\infty} (E_0[X] - E[X]) \rightarrow 0$ .  $\square$

### Appendix C. Proof for Proposition 3

Note that the difference between  $\hat{E}_0[X]$  and  $E_0[X]$  is exactly the omitted second term in (17):

$$\hat{E}_0[X] - E_0[X] = \frac{R(D,p)}{mn^{\frac{1}{D}}} \sum_{i=1}^m \left(1 - \frac{i-1}{n}\right) \left(\frac{i-1}{n}\right)^i \sum_{k=1}^{\infty} \left(\frac{i-1}{n}\right)^{k-1} \left((k+i)^{\frac{1}{D}} - i^{\frac{1}{D}}\right). \quad (\text{C.1})$$

Before presenting the proof for Proposition 3, we first introduce the following lemmas.

#### Lemma 5.

$$0 \leq \hat{E}_0[X] - E_0[X] \leq \frac{R(D,p)}{mn^{\frac{1}{D}}} \sum_{i=1}^m \left(\frac{i-1}{n}\right)^{i-1} \left(1 - \frac{i-1}{n}\right) \text{Li}_{-\frac{1}{D}}\left(\frac{i-1}{n}\right). \quad (\text{C.2})$$

*Proof.* For  $0 \leq \frac{1}{D} \leq 1, k \geq 1, i \geq 1$ , it is well-known that  $0 < (k+i)^{\frac{1}{D}} \leq k^{\frac{1}{D}} + i^{\frac{1}{D}}$ , where the right hand side equality occurs only at  $D = 1$ . As such, the following must hold from Equation (C.1):

$$0 \leq \hat{E}_0[X] - E_0[X] \leq \frac{R(D,p)}{mn^{\frac{1}{D}}} \sum_{i=1}^m \left(1 - \frac{i-1}{n}\right) \left(\frac{i-1}{n}\right)^i \sum_{k=1}^{\infty} \left(\frac{i-1}{n}\right)^{k-1} k^{\frac{1}{D}}.$$

By using  $\text{Li}_{-\frac{1}{D}}\left(\frac{i-1}{n}\right) = \sum_{k=1}^{\infty} \left(\frac{i-1}{n}\right)^k k^{\frac{1}{D}}$  to substitute the summation term completes the proof.  $\square$

**Lemma 6.** *When  $n \gg 1, n \geq m \geq 1$ , for any  $1 \leq i \leq m$ ,*

$$\left(\frac{i-1}{n}\right)^i \leq \max \left\{ \left(\frac{m-1}{n}\right)^m, e^{-4} \right\} < e^{-1}. \quad (\text{C.3})$$

*Proof.* Let  $f(i) = \left(\frac{i-1}{n}\right)^i$ , with continuous argument  $i \in [1, n]$ . Obviously,  $f(i) > 0$  for  $i \in (1, n]$  and takes its minimum value of 0 at  $i = 1$ . It has the same monotonicity and maximizer(s) as its logarithm  $g(i) = \ln f(i) = i \ln \left(\frac{i-1}{n}\right)$ . The first- and second-order derivatives of  $g(i)$  are  $g(i)' = \ln \left(\frac{i-1}{n}\right) + \frac{i}{i-1}$  and  $g(i)'' = \frac{i-2}{(i-1)^2}$ . Clearly,  $g(i)'' = 0$  at  $i = 2$ . For  $i \in (1, 2)$ ,  $g(i)'' < 0$  and for  $i > 2$ ,  $g(i)'' > 0$ . This indicates there exists at most one local maximum point  $i^* \in (1, 2)$

that satisfies the first-order condition  $g'(i^*) = 0$ . Given  $1 \leq m \leq n$ , for any  $1 \leq i \leq m$ , the local maximum of  $g(i)$  can only be at  $i^*$  or  $m$ . As such,

$$\max_{i \in [1, m]} f(i) = \max \left\{ \left( \frac{m-1}{n} \right)^m, f(i^*) \right\}.$$

Next, we examine the upper bound of  $f(i^*)$ . As  $g'(i^*) = \ln \left( \frac{i^*-1}{n} \right) + \frac{i^*}{i^*-1} = 0$ , we know  $\frac{i^*-1}{n} = e^{-\frac{i^*}{i^*-1}}$ . Substituting this result back into  $f(i^*)$ , we have

$$f(i^*) = e^{\frac{i^*2}{1-i^*}}, i^* \in (1, 2).$$

For all  $i > 1$ , function  $e^{\frac{i^2}{1-i}}$  takes its maximum value  $e^{-4}$  at  $i = 2$ . Therefore,  $f(i^*) \leq e^{-4}$ , which implies:

$$\max_{i \in [1, m]} f(i) = \max \left\{ \left( \frac{m-1}{n} \right)^m, e^{-4} \right\}.$$

When  $n \gg 1$ ,  $\left( \frac{m-1}{n} \right)^m \leq \left( \frac{n-1}{n} \right)^n$ , and it must be strictly less than  $\lim_{n \rightarrow +\infty} \left( \frac{n-1}{n} \right)^n \rightarrow e^{-1}$ .  $\square$

Now we are ready to prove Proposition 3.

**Proposition 3.** *When  $n \gg m \geq 1$ ,*

$$0 \leq \frac{\hat{E}_0[X] - E_0[X]}{\hat{E}_0[X]} \leq \max \left\{ \left( \frac{m-1}{n} \right)^m, e^{-4} \right\}.$$

and  $\lim_{n \rightarrow +\infty} \left( \hat{E}_0[X] - E_0[X] \right) \rightarrow 0$  for  $D < \infty$ .

*Proof.* From Equation (C.3), we know for all  $i \in \{1, \dots, m\}$ ,  $\left( \frac{i-1}{n} \right)^i \leq \max \left\{ \left( \frac{m-1}{n} \right)^m, e^{-4} \right\}$ . As such, the inequality in Equation (C.2) can be relaxed to:

$$0 \leq \hat{E}_0[X] - E_0[X] \leq \max \left\{ \left( \frac{m-1}{n} \right)^m, e^{-4} \right\} \frac{R(D, p)}{em^{\frac{1}{D}}} \left[ 1 + \sum_{i=2}^m \left( \frac{n}{i-1} - 1 \right) \text{Li}_{-\frac{1}{D}} \left( \frac{i-1}{n} \right) \right]. \quad (\text{C.4})$$

Dividing both sides of the inequalities in (C.4) by those in Equation (18), respectively, completes the proof of the inequalities.

Now we prove the limit. Combining Equations (C.3) and (19), the right hand side inequality in Equation (C.4) can be relaxed to:

$$\hat{E}_0[X] - E_0[X] \leq \frac{R(D, p)n^{1-\frac{1}{D}}}{em} \sum_{i=1}^m \frac{1}{n-i+1}. \quad (\text{C.5})$$

For the special case when  $m = n$ ,  $\sum_{i=1}^m \frac{1}{n-i+1}$  becomes the partial sum of the harmonic series  $\sum_{i=1}^n \frac{1}{i}$ . According to Boas Jr. and Wrench Jr. (1971), this partial sum equals  $\ln n + \gamma + \frac{1}{2n} - \varepsilon_n$ , where  $\gamma \approx 0.5772$  is the Euler–Mascheroni constant and  $0 \leq \varepsilon_n \leq \frac{1}{8n^2}$ . Therefore, the inequality

in Equation (C.5) can be written into the following:

$$\hat{\mathbb{E}}_0[X] - \mathbb{E}_0[X] \leq \frac{R(D, p)}{en^{\frac{1}{D}}} \left( \ln n + \gamma + \frac{1}{2n} \right).$$

As  $n \rightarrow +\infty$ , the L'Hôpital's rule yields:

$$\lim_{n \rightarrow +\infty} \frac{R(D, p)}{en^{\frac{1}{D}}} \left( \ln n + \gamma + \frac{1}{2n} \right) \sim \lim_{n \rightarrow +\infty} n^{-\frac{1}{D}}.$$

Clearly, the above limit converges to zero for  $D < \infty$ .

Now consider the case when  $m < n$ . We relax the summation term in Equation (C.5), as done in Equation (19), to obtain:

$$\hat{\mathbb{E}}_0[X] - \mathbb{E}_0[X] \leq \frac{R(D, p)}{e} \left( \frac{n^{1-\frac{1}{D}}}{m} \right) \ln \left( \frac{n}{n-m} \right).$$

The right hand side is non-decreasing with respect to  $m \in [1, n)$ , as its partial derivative is non-negative. As such, for  $m \in \mathbb{Z}^+$ , the above inequality can be further relaxed by setting  $m = n - 1$ :

$$\hat{\mathbb{E}}_0[X] - \mathbb{E}_0[X] \leq \frac{R(D, p)}{e} \left( \frac{n^{1-\frac{1}{D}} \ln n}{n-1} \right).$$

The limit of the right hand side satisfies:

$$\lim_{n \rightarrow +\infty} \frac{R(D, p)}{e} \left( \frac{n^{1-\frac{1}{D}} \ln n}{n-1} \right) \sim \lim_{n \rightarrow +\infty} n^{-\frac{1}{D}}.$$

Clearly, the above limit also converges to zero when  $D < \infty$ . This completes the proof. □